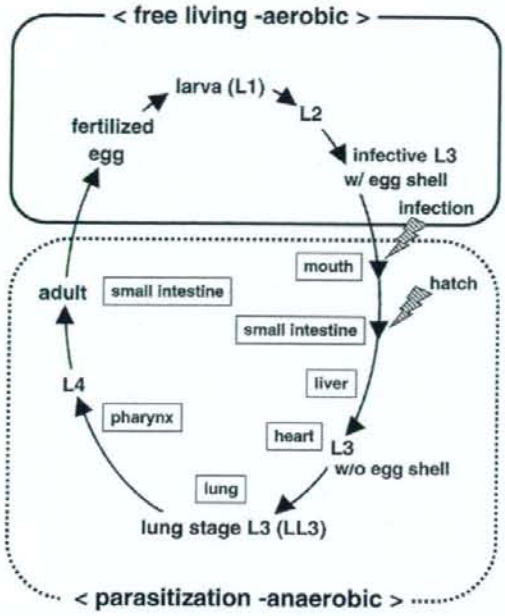

Fig. 1. Life cycle of *Ascaris suum*. Fertilized eggs grow to infective L3 under aerobic environment. Infective L3 larvae are ingested by the host, reach the small intestine and hatch there. Afterwards, larvae migrate into the host body (liver, heart, lung, pharynx), and finally migrate back to the small intestine and become adults. In the host small intestine, the oxygen concentration is only 2.5 to 5% of that of the exogenous environment [12]. w/, with; w/o, without.

succinate pathway. In the first step in the PEPCK-succinate pathway, PEPCK fixes CO_2 to PEP in the cytosol, to form oxaloacetate. This oxaloacetate is then reduced to malate, which is dismutated in mitochondria. Then, fumarate hydratase converts the malate to fumarate, which is reduced by the quinol–fumarate reductase (QFR) activity of complex II; in aerobic respiration, complex II catalyzes oxidation of succinate (succinate–ubiquinone reductase; SQR) in the mitochondria. The last step of the PEPCK-succinate pathway involves the NADH–fumarate reductase system, which is composed of complex I (NADH–quinone reductase), low-potential rhodoquinone (RQ) and complex II (QFR) [3,8]. Electron transfer from NADH to fumarate is coupled to ATP synthesis by site I phosphorylation in complex I. The difference in redox potential between NAD^+/NADH ($Em' = -320$ mV) and fumarate/succinate ($Em' = +30$ mV) is sufficient to drive ATP synthesis.

In eukaryotes, complex II is localized in the inner mitochondrial membrane, and is generally composed of 4 peptides [3]. The largest flavoprotein (Fp) subunit has an approximate molecular mass of 70 kDa and contains flavin adenine dinucleotide (FAD) as a prosthetic group. The relatively hydrophilic catalytic region of complex II is formed by the Fp subunit and the iron–sulfur cluster (Ip) subunit, whose molecular weight is about 30 kDa. The remaining subunits comprise cytochrome *b*, which contains heme *b*. Cytochrome *b* is composed of 2 hydrophobic membrane-anchoring polypeptide subunits; the 15-kDa large subunit (CybL) and the 13-kDa small subunit (CybS). These cytochrome *b* subunits are necessary for interaction between complex II and hydrophobic membrane-associated quinones such as ubiquinone (UQ) and RQ. However, it is unclear how heme *b* is involved in the electron transfer between complex II and quinones.

In a previous study, we showed that *A. suum* mitochondria express stage-specific isoforms of complex II [5,6,9]. While there is no difference in the isoforms of the Ip and CybL subunits of complex II between L3 larvae and adult *A. suum*, they have different isoforms of the complex II subunits Fp (larval, Fp^L; adult, Fp^A) and CybS (larval, $CybS^L$; adult, $CybS^A$). Quinone species in the mitochondria also change during the life cycle of *A. suum*. In adult mitochondria, the predominant quinone is the low-potential rhodoquinone (RQ; $Em' = -63$ mV); in larvae, the predominant quinone is ubiquinone (UQ; $Em' = +110$ mV) [10]. A combination of SQR and UQ, and that of QFR and a low-potential quinone, such as RQ or menaquinone (MK), is also observed in *E. coli* and other bacteria during metabolic adaptation to changes in oxygen supply [11]. UQ has a higher potential than RQ; therefore, RQ is better suited to transferring electrons to fumarate than is UQ. In L2 and L3 *A. suum* larvae, UQ preferentially donates electrons to the cytochrome chain in the mitochondria. Thus, UQ participates in aerobic metabolism in *A. suum* larvae, whereas RQ participates in anaerobic metabolism in adult *A. suum*.

After ingestion by the definitive host, the L3 larvae penetrate the intestinal wall and reach to the lung migrating through the tissues such as liver and heart. The L3 larvae passes from lung via the trachea to the small intestine where they molt to L4 and develop into sexually maturate adult worms in the small intestine [12]. Although studies have shown a clear difference in energy metabolism between larval and adult *A. suum* mitochondria, little is known about changes in the properties of mitochondria (including respiration) during migration of *A. suum* larvae in the host.

In the present study, we examined changes in subunit composition of *A. suum* larval complex II from lung stage L3 (LL3) larvae obtained from rabbits. Enzymatic analyses showed that properties of LL3 mitochondria differed from those of L3 and adult mitochondria. Protein chemical analysis revealed that the change in complex II begins with the anchor CybS subunit, and then occurs in the Fp subunit.

2. Materials and methods

2.1. Parasites

A. suum adult worms were procured from a slaughterhouse in Tokyo, Japan. Third stage infective (L3) larvae and lung stage L3 (LL3) larvae were obtained as previously described [5,13]. All animals used in this study were acclimatized to the experimental conditions for 2 weeks before the experiment. Animal experiments were conducted in accordance with the protocols approved by the Animal Care and Use Committee, National

Institute of Animal Health (Approval nos. 589,712). For the preparation of LL3 larvae, Japanese white rabbits were made to ingest infective *A. suum* eggs (approximately 1.5×10^5 eggs per rabbit), and infected lungs were removed from the rabbits 7 days after ingestion of the eggs. The lungs were cut into 2-cm cubes using a razor blade, and the cubes were put into nylon mesh bags (KA1000, Eiken Kizai, Tokyo, Japan) in 50-ml polypropylene conical tubes filled with phosphate-buffered saline (PBS) containing 100 μg/ml penicillin and 100 μg/ml streptomycin. Those tubes were then kept in a humidified incubator at 37 °C for 4 to 5 h. During that incubation, the larvae dropped out of the bags into the bottom of the tubes. The larvae were then washed several times with fresh PBS in a 37 °C water bath. Contaminating erythrocytes from the host rabbits were eliminated by hemolysis, which was induced by washing the pellet containing LL3 larvae with pre-warmed tap water at 37 °C. The body length of the LL3 larvae, obtained from infected rabbit on day 7 post-infection, were 1.2–1.3 mm. They were slightly smaller than LL3 larvae derived from infected swine at the same post-infectious stage (1.5 mm) [14].

2.2. Preparation of mitochondria from L3, LL3 and adult A. suum

Mitochondria from L3 and adult *A. suum* muscle were prepared using the method described by Amino et al. [5]. Because that method was not applicable to LL3 mitochondria, we established the following method to obtain active mitochondria from LL3; the entire procedure was performed on ice or at 4 °C. The LL3 larvae were gently suspended in an equal volume of ice-cold suspension buffer containing 210 mM mannitol, 10 mM sucrose, 1 mM disodium EDTA and 50 mM Tris–HCl (pH 7.5), supplemented with 10 mM sodium malonate [15]. The LL3 larvae in the suspension were cut using a scalpel (No. 10 blade, Feather, Osaka, Japan) on a 90 × 75 × 3-mm custom-made glass plate with a hollow (diameter, 22 mm; depth, 3 mm) in the middle. The cut larvae were then homogenized with a hand-powered glass–glass homogenizer for 15 min, and the homogenate was centrifuged at 500 × g for 1 min. The resulting supernatant was centrifuged at 10,000 × g for 10 min to obtain the mitochondrial pellet. The pellet was resuspended in the suspension buffer and stored at −80 °C until used. The protein concentration of the mitochondria was determined using the method of Lowry [16], using bovine serum albumin as the standard.

2.3. Enzyme assay

All assays were performed at 25 °C, using 50 mM potassium phosphate (pH 7.5) as the reaction buffer. The SQR [17], succinate dehydrogenase (SDH) [18], QFR [19] and NADH–fumarate reductase [8] activities of mitochondria were assayed as described. The NADH-decyl UQ (-dUQ) and NADH-decyl RQ (-dRQ) assays were performed using the same method as the NADH–fumarate reductase activity assay, except that 60 μM dUQ or dRQ was used as the electron acceptor, instead of sodium fumarate.

2.4. Quantitative analysis of quinone in LL3 mitochondria

Quinones were extracted from lyophilized LL3 mitochondria, and were analyzed by reverse-phase HPLC as described by Miyadera et al. [20]. The concentrations of quinones were determined spectrophotometrically using the following extinction coefficients: for UQ, $E_{1\%1\ cm}$ at 275 nm = 158; for RQ, $E_{1\%1\ cm}$ at 283 nm = 141 [10].

2.5. Western blotting

Complex II from L3, LL3 and adult mitochondria was analyzed by Western blotting using the method of Towbin et al. [21]. The mitochondrial proteins were separated by SDS-PAGE, using a 7.5% acrylamide gel for the Fp subunit, and using a 10/20% gradient acrylamide gel (Daiichi, Tokyo, Japan) for the Ip and CybS subunits. The proteins were then transferred to a nitrocellulose membrane at 4 °C and 80 V for 1 h. The membranes were incubated with the following antibodies in Tris-buffered saline containing 0.05% (w/v) Tween 20 (TBST) and 2% (w/v) skim milk: anti-Fp monoclonal, diluted 1:3000 [18]; anti-$CybS^A$ monoclonal, diluted 1:5000 [5]; $CybS^L$ peptide-based polyclonal, diluted 1:300 [5]; mixture of anti-Ip and anti-CybS polyclonal, diluted 1:2000 [5]. Each membrane was then incubated for 30 min with one of the following alkaline phosphatase-conjugated secondary antibodies: goat anti-mouse IgG (for Fp and $CybS^A$), or goat anti-rabbit IgG (for $CybS^L$, Ip and CybS). The proteins were detected using the alkaline phosphatase method. The amount of protein was normalized to the intensity of the Ip subunit at each stage, using NIH Image (a free image analyzing program for the Macintosh, developed by National Institutes of Health (NIH); www.rsb.info.nih.gov/nih-image/download.html).

2.6. Solubilization of mitochondria for blue native (BN-) PAGE

Mitochondria from L3, LL3 and adult *A. suum* (1.5 μmol/min in SDH activity) were incubated on ice for 1 h in 0.5% (w/v) sucrose monolaurate (SML) and Native PAGE™ sample buffer containing 50 mM Bis–Tris, 6 N HCl, 50 mM NaCl, 10% (w/v) glycerol and 0.001% (w/v) Ponceau S in 10 mM Tris–HCl (pH 7.5) (User manual, version A 2006; www.invitrogen.com/content/sfs/manuals/nativepage_man.pdf, Invitrogen, Carlsbad, CA, USA). They were then ultracentrifuged at 200,000 × g and 4 °C for 1 h, and the resulting supernatant was subjected to BN-PAGE, as described below.

2.7. BN-PAGE, CBB staining, in-gel SDH activity staining and Western blotting

The solubilized mitochondria were subjected to BN-PAGE [22] using Native PAGE Novex 4–16% Bis–Tris gels (Invitrogen). Electrophoresis was performed at 4 °C, at 150 V for 1 h, and then at 250 V, voltage constant. The cathode and anode buffers were prepared according to the user's manual of the Native PAGE Novex Bis–Tris gel system. Following the BN-PAGE, CBB staining was performed according to the user's

manual. The SDH activity of mitochondrial protein of L3, LL3 and adult *A. suum* was detected as described elsewhere [18,23]. After the BN-PAGE (first dimension), the gel cut by lane from the first-dimensional gel was equilibrated with SDS-PAGE buffer, and was then loaded onto the second-dimensional gel (7.5% acrylamide gel for Fp, and 10/20% gradient acrylamide gels (Daiichi) for Ip and CybS). The subsequent analysis by Western blotting was performed as described above.

3. Results

3.1. Enzymatic properties of LL3 complex II

Because only a small amount of LL3 larvae was obtained, and because LL3 larvae were more resistant to homogenization than L3 larvae and adult worms, we tried to establish a specific and reproducible protocol for the preparation of mitochondria from LL3 larvae. We found that cutting LL3 larvae with a scalpel was an effective method of recovering active mitochondria. Using the established protocol, we obtained approximately 0.5 mg of mitochondria from 1 infected rabbit. Fig. 2 shows the results of comparative analysis of enzyme activities, relative to NADH–fumarate reductase activity, in L3, LL3 and adult mitochondria.

The Fp and Ip subunits form the hydrophilic catalytic portion of complex II, and act as a succinate dehydrogenase (SDH), catalyzing the oxidation of succinate by the water-soluble electron acceptor phenazine methosulfate. The L3 and LL3 mitochondria had almost identical levels of SDH activity, whereas the SDH activity of adult mitochondria was 2.7 to 3.9 times higher than that of L3 and LL3 mitochondria (Fig. 2A). SQR catalyzes electron transfer from succinate to the physiological electron acceptor, ubiquinone. Similarly, SQR activity of adult mitochondria was 1.8 to 3.9 times higher than that of L3 and LL3 mitochondria (Fig. 2B). QFR catalyzes a reaction that is the reverse of the reaction catalyzed by SQR. The QFR activity of LL3 mitochondria was higher than that of L3 and adult mitochondria (Fig. 2C). The NADH–fumarate

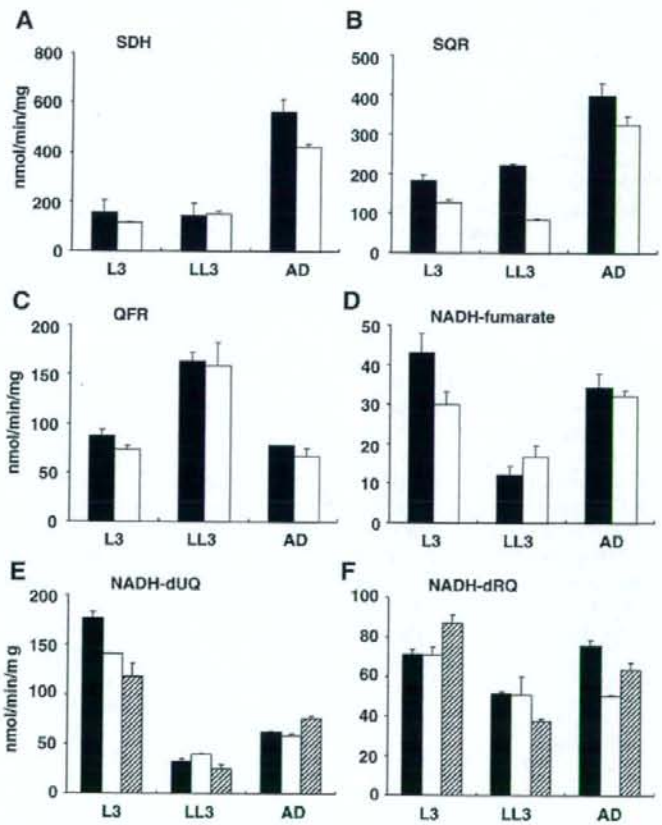

Fig. 2. Enzyme assay. Enzyme activities of complex I and II of mitochondria from L3 *A. suum* larvae, LL3 *A. suum* larvae, and *A. suum* adults. (A) SDH, (B) SQR, (C) QFR, (D) NADH–fumarate reductase, (E) NADH-dUQ and (F) NADH-dRQ. The mean and standard error were derived from triplicate measurements. Solid bars indicate experiment 1; open bars indicates experiment 2; stripe bars indicate experiment 3. Assays were performed as in materials and methods.

reductase system is an anaerobic electron-transport system of mitochondria, and is the terminal step of the PEPCK-succinate pathway. In the NADH–fumarate reductase system, the reducing equivalent of NADH is transferred to the low-potential RQ by the NADH-RQ reductase complex (Complex I). This pathway ends with the production of succinate by the rhodoquinol-fumarate reductase activity of complex II. Unexpectedly, the NADH–fumarate reductase activity of LL3 mitochondria was lower than that of L3 and adult mitochondria (Fig. 2D). The NADH-dUQ and NADH-dRQ activities of LL3 mitochondria were lower than those of L3 and adult mitochondria (Fig. 2E and F), suggesting that the low NADH–fumarate reductase activity of LL3 mitochondria is due to the lower activity of complex I in LL3 mitochondria.

3.2. Quinone components in LL3 mitochondria

Because quinone species are important low-molecular-weight mediators of electron transfer between respiratory enzymes, and because the ratio between RQ and UQ seems to be a critical factor in the direction of electron transfer in the chain, we examined the quinone content of LL3 mitochondria complex II. Although the amount of LL3 mitochondria that we obtained was quite limited, we performed the analysis using 2 different samples of LL3 mitochondria. The first sample of LL3 mitochondria contained 1.68 nmol/mg UQ-9 and 0.85 nmol/mg RQ-9. A similar result was obtained for the second sample (Table 1), indicating that the UQ content of LL3 mitochondria is approximately 2-fold greater than that of RQ. It should be noted that UQ-9 is the predominant quinone of L3 complex II (75% of the total quinone content), and that RQ is the only quinone present in complex II from adult *A. suum* muscle [10].

3.3. Subunit composition of the LL3 mitochondria complex II

To examine the subunit structure of complex II in LL3 mitochondria, we performed Western blotting. Because the isoforms of the Ip and CybL subunits do not change during the *A. suum* life cycle [5], the amount of proteins used for the Western blotting of Fp and CybS subunits was normalized to the intensity of the Ip subunit, which was visualized using the alkaline phosphatase method (Fig. 3D). LL3 mitochondrial complex II contained both Fp^L and Fp^A (Fig. 3). The LL3 and adult complex II had a Fp^L:Fp^A band intensity ratio of 1:0.56 and 1:3.5, respectively, whereas only the Fp^L band was observed in blots of L3 complex II (Fig. 3A). For the $CybS^A$ subunit, the

Table 1
Quinone quantitative analysis of LL3 mitochondria

Experiment	(nmol/mg)		Ratio
	UQ-9[a]	RQ-9[b]	UQ-9[a]:RQ-9[b]
1	1.68	0.85	1.98:1
2	1.89	1.00	1.89:1

[a] UQ-9, ubiquinone-9.
[b] RQ-9, rhodoquinone-9.

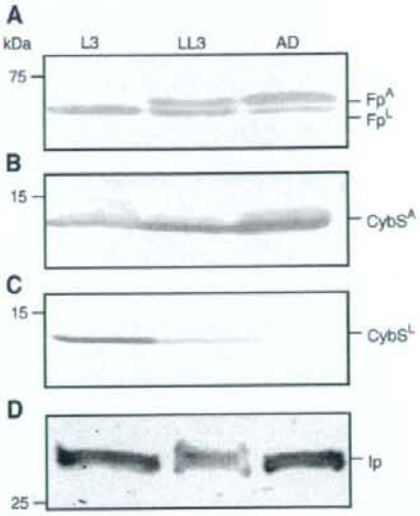

Fig. 3. Western blotting. Western blotting with (A) *A. suum* Fp monoclonal antibody, diluted 1:3000. (B) Monoclonal antibody against $CybS^A$ diluted 1:5000, and (C) Peptide-based polyclonal antibody against $CybS^L$ diluted 1:300. Protein levels were normalized to the Ip band intensity using (D) mixture of anti-Ip and anti-CybS polyclonal antibody diluted 1:2000. L3, *A. suum* larvae prepared from embryonated eggs; LL3, lung-stage L3; AD, *A. suum* adult. Precision Plus All Blue Standard (BIO-RAD).

L3:LL3:adult band intensity ratio was 1:3.5:6.1 (Fig. 3B). Only a small amount of $CybS^L$ was detected in LL3 mitochondria (<5% of $CybS^L$ in L3 mitochondria), and no $CybS^L$ was found in adult mitochondria (Fig. 3C). This result was reproducible in more than 3 experiments, suggesting that the subunit isoform change of LL3 complex II starts with CybS, and then occurs in Fp.

Because Western blotting clearly showed a difference in timing of isoform change between Fp and CybS subunits during migration in the host, we used BN-PAGE to examine the subunit composition of functional complex II. Mitochondrial proteins of each stage solubilized with sucrose monolaurate were subjected to BN-PAGE, and were then stained for CBB (Fig. 4A) or SDH activity (Fig. 4B) in the gel. Complex II from all 3 stages exhibited SDH activity in the gel, and band intensities of the 3 stages were almost identical when the amount of protein was normalized to 1.5 μmol/min SDH activity.

Next, we performed two-dimensional electrophoresis; with BN-PAGE as the first dimension, and SDS-PAGE as the second dimension. After the BN-PAGE, the gel was cut and was horizontally loaded onto SDS-PAGE. Following the two-dimensional electrophoresis, proteins were analyzed by Western blotting (Fig. 4C). Spots of Fps and CybSs were found in the same position as the SDH-stain band, indicating that native complex II with 4 subunits migrated during electrophoresis in the presence of the detergent. No extra spot was found in an area different from the SDH-stain position. In addition, the patterns

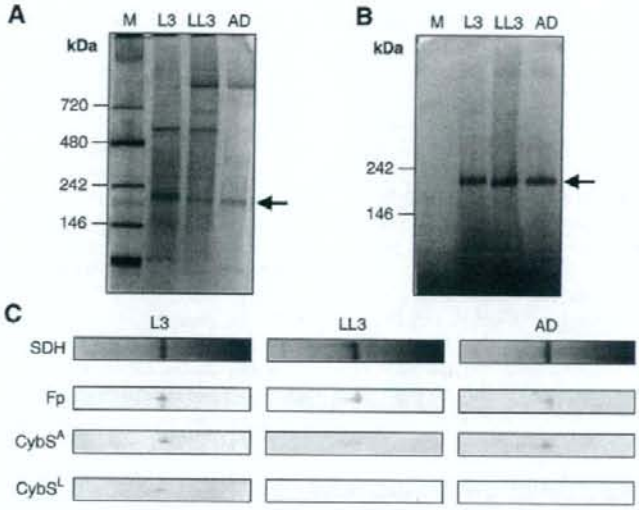

Fig. 4. BN-PAGE analysis. BN-PAGE analysis of mitochondria from *A. suum* L3 larvae, LL3 larvae and adults (1.5 μmol/min SDH activity). (A) CBB-stain. Arrow indicates expected SDH active bands. (B) SDH activity stained in gels of Native PAGE™ Bis–Tris gel (4–16%). Arrow shows SDH active bands. (C) Western blotting after SDS-PAGE, following BN-PAGE. Antibodies used were the same as in Fig. 3. The size marker is Native Mark Unstained Protein Standard (Invitrogen).

of intensity of the spots in Fig. 4C were almost identical to the results of Western blotting after SDS-PAGE (Fig. 3).

4. Discussion

In the present study, biochemical analyses of mitochondrial complex II were performed to elucidate how complex II in *A. suum* mitochondria change its isoform composition during migration in the mammalian host. In the first step of this study, we examined complex II from LL3 larvae (Fig. 1), because there is an established method of sample collection from rabbit lung, and because several properties of LL3 have been well studied [13,24]. The natural host of *A. suum* is swine so that we need pigs for developing the migratory phase and the adult stages. However, pig rearing facilities are currently quite limited for the purpose of doing *Ascaris* infection. Helminth researchers have previously examined the life cycle and worm burdens in rabbits [25,26]. The results showed that several criteria such as the organ migratory routes and recovery of larvae in rabbits were quite similar to those in pigs, indicating that rabbit can be fairly used for permissive hosts. Actually, *Ascaris* researchers including our group have employed rabbits to do biochemical experiments of the roundworms [27,28].

We previously demonstrated that *A. suum* mitochondria express stage-specific isoforms of complex II; i.e., the flavoprotein subunit (Fp) and the small subunit of cytochrome *b* (CybS) of complex II isolated from L3 infective eggs differ from those of adult muscle complex II, while the 2 forms of complex II have an identical iron-sulfur cluster subunit (Ip) and large subunit of cytochrome *b* (CybL). Therefore, the subunit isoform composition of complex II must change during migration in the host. To our surprise, Western blot analyses showed that both the Fp^L and Fp^A isoforms (in the ratio of 1: 0.56) were present in LL3 mitochondria, while the majority of CybS subunit was of the isoform $CybS^A$ (Fig. 3A and B). This means that expression of adult Fp does not synchronize with that expression of adult CybS, and suggests that LL3 complex II has a different combination of subunit isoforms than L3 and adult complex II.

To analyze the native state of complex II subunit composition in LL3 mitochondria, we used BN-/SDS-PAGE two-dimensional electrophoresis (Fig. 4C). The spots of the subunits were found at the same position as the SDH bands,

Table 2
Enzyme activities of L3, LL3 and adult complex I and II of *Ascaris suum* mitochondria

		Specific activity (nmol/min/mg)		
Assay	Experiment	L3	LL3	Adult
SDH	1	158±36	145±16	566±15
(complex II)	2	118±5.6	152±25	424±22
SQR	1	184±28	224±8.3	400±63
(complex II)	2	129±16	84.1±4.0	326±43
QFR	1	87.8±6.0	164±8.6	78.5±0.058
(complex II)	2	73.5±7.6	159±47	66.8±16
NADH–fumarate	1	43.0±10	12.3±4.4	34.4±7.1
reductase (complex I,II)	2	30.1±6.4	16.7±5.6	32.3±2.6
NADH-dUQ	1	177±12	32.3±5.6	62.4±1.9
	2	141±0.92	39.8±1.9	58.6±4.6
(complex I)	3	118±26	24.8±8.8	76.3±4.9
NADH-dRQ	1	71.4±4.4	51.6±2.0	75.7±5.6
	2	71.0±7.8	51.0±18	50.3±1.3
(complex I)	3	87.1±8.5	37.6±2.4	63.4±7.6

without any extra spots. This result indicates that the spots detected were derived from active complex II consisting of 4 subunits. In LL3 mitochondria, all 4 larva-/adult-types of Fp-CybS subunits was observed, while Fp^L, $CybS^A$ and $CybS^L$ subunit isoforms were detected in L3 mitochondria, and Fp^L, Fp^A and $CybS^A$ subunit isoforms were detected in adult mitochondria. The pattern of the intensity of the spots in Fig. 4C is consistent with that of the Western blotting after SDS-PAGE (Fig. 3), indicating that mitochondrial complex II subunit switching first occurs in CybS, and then occurs in Fp, during migration in the host.

Of the 4 possible Fp-CybS subunit combinations (Fp^L-$CybS^A$, Fp^A-$CybS^A$, Fp^L-$CybS^L$ and Fp^A-$CybS^L$), Fp^L-$CybS^A$ is the predominant combination in LL3 mitochondria. Western blot analysis of young adult mitochondria obtained from the muscle of 12-cm-long female worms showed that $CybS^L$ had completely disappeared, whereas Fp^L remained at a ratio of Fp^L:Fp^A = 1:1.5 (data not shown), although only 1 SDH band was observed in BN-PAGE. This finding may be due to similar properties between the 2 complexes with different combinations.

However, several questions remain unanswered. Because of limited sample amount, it is difficult to purify complex II from LL3 mitochondria. Reports indicate that adult *A. suum* uses the NADH–fumarate reductase system in its anaerobic host environment; in the NADH–fumarate reductase system, the QFR activity of mitochondrial complex II plays a significant role [3,29,30]. However, we previously found that L3 complex II had higher QFR activity than adult complex II, and presumed that this was due to pre-adaptation to the dramatic change in oxygen availability during infection of the host [5]. In the present study, we found that the QFR activity of LL3 complex II was twice as high as that of L3 complex II (Fig. 2C, Table 2). The host lung is a relatively aerobic environment (13.2% O_2) [31], suggesting that the larvae pre-adapt before they migrate into the anaerobic environment of the host small intestine (5% O_2).

Although LL3 mitochondria showed the highest QFR activity of the 3 stages we examined, their NADH–fumarate reductase activity was unexpectedly low (Fig. 2D). This appears to be due to the effects of low complex I activity, as indicated by the NADH-dUQ and NADH-dRQ assays (Fig. 2E and F). The NADH–fumarate reductase system is composed of complex I (initial dehydrogenase of NADH), RQ (electron mediator), and complex II (terminal oxidase for fumarate reduction). We also examined the quinone content of the mitochondria. Analysis of the quinone contents of mitochondria isolated from unembryonated eggs, L3 larvae and adult muscle showed that the predominant quinone in larval mitochondria (which possess an aerobic respiratory chain) was UQ-9 (75% of the total quinone content) [10]. In contrast, the only quinone present in anaerobic mitochondria from adult muscle is RQ-9. Consistent with these findings, reconstitution studies using bovine heart complex I and adult *A. suum* QFR show that RQ is essential for the function of the NADH–fumarate reductase system [32]. Specifically, when RQ-9 was incorporated into the system, the maximum activity of reconstituted NADH–fumarate reductase activity was 430 nmol/min/mg of *A. suum* complex II, while no activity was observed in the presence of UQ-9. In addition, our previous findings suggest that although *A. suum* adult complex I uses both RQ and UQ as electron acceptors, the 2 quinones have different ways of binding reaction and reaction with *A. suum* complex I [33]. It should be noted that in the present study, UQ accounted for 66% of the total quinone of LL3 complex II, which is an intermediate between those of L3 and adult complex II [10]. Further analysis of the effect of endogenous quinones in the mitochondria of the enzyme activities of complex I and complex II is needed to elucidate the unique properties of the NADH–fumarate reductase system of *A. suum*.

In the present study, we examined how mitochondrial complex II of *A. suum* changes its subunit composition, especially during migration in the host. We found that the small subunit of cytochrome *b* (CybS) starts to change its isoform before the flavoprotein (Fp) subunit does so. Further clarification of this process will require analysis of larvae from other migration stages in the host. In each stage, the metabolic pathway of *A. suum* may continue to change according to the environmental changes, even in the host body. To elucidate this dynamic change in the mitochondrial respiratory system of *A. suum* during migration, we plan to establish an experimental system using swine, which is a definitive host of *A. suum*. With such a system, further biochemical analysis should reveal novel properties of complex II in LL3 mitochondria.

Acknowledgements

We thank Dr. Tetsuro Ishii for his academic support. This study was supported by a grant-in-aid for scientific research on Priority Areas, for the 21st Century COE Program (F-3) and for Creative Scientific Research from the Japanese Ministry of Education, Science, Culture, Sports and Technology (180 73004, 18GS0314).

References

[1] Komuniecki R, Komuniecki PR. Aerobic–anaerobic transitions in energy metabolism during the development of the parasitic nematode *Ascaris suum*. In: Boothroyd JC, Komuniecki R, editors. Molecular approaches to parasitology. New York: Wiley-Liss; 1995.

[2] Tielens AGM, Rotte C, van Hellemond JJ, Martin W. Mitochondria as we don't know them. Trends Biochem Sci 2002;27:56–72.

[3] Kita K, Takamiya S. Electron-transfer complexes in *Ascaris* mitochondria. Adv Parasitol 2002;51:95–131.

[4] Kita K. Electron-transfer complexes in *Ascaris suum*. Parasitol Today 1992;8: 155–9.

[5] Amino H, Osanai A, Miyadera H, Shinjyo N, Tomitsuka E, Taka H, et al. Isolation and characterization of the stage-specific cytochrome *b* small subunit (CybS) of *Ascaris suum* complex II from the aerobic respiratory chain of larval mitochondria. Mol Biochem Parasitol 2003;128: 175–86.

[6] Amino H, Wang H, Hirawake H, Saruta F, Mizuchi D, Mineki R, et al. Stage-specific isoforms of *Ascaris suum* complex II: the fumarate reductase of the parasitic adult and the succinate dehydrogenase of free-living larvae share a common iron–sulfur subunit. Mol Biochem Parasitol 2000;106: 63–76.

[7] Kita K, Hirawake H, Miyadera H, Amino H, Takeo S. Role of complex II in anaerobic respiration of the parasite mitochondria from *Ascaris suum* and *Plasmodium falciparm*. Biochim Biophys Acta 2002;1553: 123–39.

[8] Omura S, Miyadera H, Ui H, Shiomi K, Yamaguchi Y, Masuma R, et al. An anthelmintic compound, nafredin, shows selective inhibition of

complex I in helminth mitochondria. Proc Natl Acad Sci U S A 2001;98: 60–2.
[9] Saruta F, Kuramochi T, Nakamura K, Takamiya S, Yu Y, Aoki T, et al. Stage-specific isoforms of complex II (succinate–ubiquinone oxidoreductase) in mitochondria from the parasitic nematode, *Ascaris suum*. J Biol Chem 1995;270:928–32.
[10] Takamiya S, Kita K, Wang H, Weinstein PP, Hiraishi A, Oya H, et al. Developmental changes in the respiratory chain of *Ascaris* mitochondria. Biochim Biophys Acta 1993;1141:65–74.
[11] Cole ST, Condon C, Lemire BD, Weiner JH. Molecular biology, biochemistry and bioenergetics of fumarate reductase, a complex membrane-bound iron-sulfur flavoenzyme of *Escherichia coli*. Biochim Biophys Acta 1985;811: 381–403.
[12] Heinz M. Encyclopedic reference of parasitology. 2nd ed. Berlin: Springer; 2001.
[13] Islam MK, Miyoshi T, Yamada M, Alim MA, Huang X, Motobu M, et al. Effect of piperazine (diethylenediamine) on the moulying proteome express and pyrophosphate activity of *Ascaris suum* lung-stage larvae. Acta Trop 2006;99:208–17.
[14] Miyazaki I. Helminthic zoonoses. Tokyo: International Medical Foundation of Japan; 1991. p. 295–305.
[15] Takamiya S, Furushima R, Oya H. Electron transfer complexes of *Ascaris suum* muscle mitochondria I. Characterization of NADH-cytochrome *c* reductase (complex I–III), with special reference to cytochrome localization. Mol Biochem Parasitol 1984;13: 121–34.
[16] Lowry OH, Rosebrough NJ, Farr AL, Randall RJ. Protein measurement with the folin phenol reagent. J Biol Chem 1951;193:265–75.
[17] Miyadera H, Shiomi K, Ui H, Yamaguchi Y, Masuma R, Tomoda H, et al. Atopenins, potent and specific inhibitors of mitochondrial complex II (succinate–ubiquinone oxidoreductase). Proc Natl Acad Sci U S A 2003;100: 473–7.
[18] Tomitsuka E, Goto Y, Taniwaki M, Kita K. Direct evidence for expression of Type II flavoprotein subunit in human complex II (succinate–ubiquinone reductase). Biochem Biophys Res Commun 2003;311: 774–9.
[19] Kita K, Vibat CR, Meinhardt S, Guest JR, Gennis RB. One-step purification from *Escherichia coli* of complex II (succinate:ubiquinone oxidoreductase) associated with succinate-reducible cytochrome b_{556}. J Biol Chem 1989;264:2672–7.
[20] Miyadera H, Amino H, Hiraishi A, Taka H, Murayama K, Miyoshi H, et al. Altered quinone biosynthesis in the long-lived *clk-1* mutants of *Caenohabditis elegans*. J Biol Chem 2001;276:7713–6.
[21] Towbin H, Staehelin T, Gorton J. Electrophoretic transfer of proteins from polyacrylamide gels to nitrocellulose sheets: procedure and some applications. Proc Natl Acad Sci U S A 1979;76: 4350–4.
[22] Shägger H, Cramer WA, von Jagow G. Analysis of molecular mass and oligomeric states of protein complexes by blue native electrophoresis and isolation of membrane protein complexes by two-dimensional native electrophoresis. Anal Biochem 1994;217:220–30.
[23] Kho CW, Park SG, Lee DH, Cho S, Oh GT, Kang S, et al. Activity staining of glutathione peroxidase after two-dimensional gel electrophoresis. Mol Cell 2004;18:369–73.
[24] Geenen PL, Bresciani J, Boes J, Pedersen A, Eriksen L, Fagerholm HP, et al. The morphogenesis of *Ascaris suum* to the infective third-stage larvae within the egg. J Parasitol 1999;85:616–22.
[25] Jeska EL, Williams JF, Cox DF. *Ascaris suum*: larval returns in rabbits, Guinea pigs and mice after low-dose exposure to eggs. Exp Parasitol 1969;26: 187–92.
[26] Stormberg BE, Soulsby EJL. *Ascaris suum*: immunization with soluble antigens in the Guinea pig. Int J Parasitol 1977;7:287–91.
[27] Komuniecki PR, Vanover L. Biochemical changes during the aerobic–anaerobic transition in *Ascaris suum* larvae. Mol Biochem Parasitol 1987;22(2–3):241–8.
[28] Islam MK, Miyoshi T, Kasuga-Aoki H, Isobe T, Arakawa Y, Matsumoto Y, et al. Inorganic pyrophosphatase in the roundworm *Ascaris* and its role in the development and molting process of the larval stage parasites. Eur J Biochem 2003;270: 2814–26.
[29] Kita K, Shiomi K, Omura S. Advances in drug discovery and biochemical studies. Trends Parasitol 2007;23:223–9.
[30] Kuramochi T, Hirawake H, Kojima S, Takamiya S, Furushima R, Aoki T, et al. Sequence comparison between the flavoprotein subunit of the fumarate reductase (complex II) of the anaerobic parasitic nematode, *Ascaris suum* and the succinate dehydrogenase of the aerobic, free-living nematode, *Caenorhabditis elegans*. Mol Biochem Parasitol 1994;68: 177–87.
[31] Martini FH, Ober WC, Garrison CW, Welch K, Hutching RT. Fundamentals of anatomy and physiology. 4th ed. Upper Saddle River, New Jergy: Prentice Hall; 1998.
[32] Kita K, Takamiya S, Furushima R, Ma YC, Suzuki H, Ozawa T, et al. Electron-transfer complexes of *Ascaris suum* muscle mitochondria. III. Composition and fumarate reductase activity of complex II. Biochim Biophys Acta 1998;935: 130–40.
[33] Yamashita T, Ino T, Miyoshi H, Sakamoto K, Osanai A, Nakamaru-Ogiso E, et al. Rhodoquinone reaction site of mitochondrial complex I, in parasitic helminth, *Ascaris suum*. Biochim Biophys Acta 2004;1608: 97–103.

ANTIMICROBIAL AGENTS AND CHEMOTHERAPY, Jan. 2008, p. 164–170 Vol. 52, No. 1
0066-4804/08/$08.00+0 doi:10.1128/AAC.00378-07

Anaerobic NADH-Fumarate Reductase System Is Predominant in the Respiratory Chain of *Echinococcus multilocularis*, Providing a Novel Target for the Chemotherapy of Alveolar Echinococcosis▽

Jun Matsumoto,[1] Kimitoshi Sakamoto,[2]* Noriko Shinjyo,[2] Yasutoshi Kido,[2] Nao Yamamoto,[1] Kinpei Yagi,[3] Hideto Miyoshi,[4] Nariaki Nonaka,[1] Ken Katakura,[1] Kiyoshi Kita,[2] and Yuzaburo Oku[1]

Laboratory of Parasitology, Department of Disease Control, Graduate School of Veterinary Medicine, Hokkaido University, Sapporo, Japan[1]; Department of Biomedical Chemistry, Graduate School of Medicine, University of Tokyo, Tokyo, Japan[2]; Department of Medical Zoology, Hokkaido Institute of Public Health, Sapporo, Japan[3]; and Division of Applied Life Sciences, Graduate School of Agriculture, Kyoto University, Kyoto, Japan[4]

Received 20 March 2007/Returned for modification 21 June 2007/Accepted 10 October 2007

Alveolar echinococcosis, which is due to the massive growth of larval *Echinococcus multilocularis*, is a life-threatening parasitic zoonosis distributed widely across the northern hemisphere. Commercially available chemotherapeutic compounds have parasitostatic but not parasitocidal effects. Parasitic organisms use various energy metabolic pathways that differ greatly from those of their hosts and therefore could be promising targets for chemotherapy. The aim of this study was to characterize the mitochondrial respiratory chain of *E. multilocularis*, with the eventual goal of developing novel antiechinococcal compounds. Enzymatic analyses using enriched mitochondrial fractions from *E. multilocularis* protoscoleces revealed that the mitochondria exhibited NADH-fumarate reductase activity as the predominant enzyme activity, suggesting that the mitochondrial respiratory system of the parasite is highly adapted to anaerobic environments. High-performance liquid chromatography–mass spectrometry revealed that the primary quinone of the parasite mitochondria was rhodoquinone-10, which is commonly used as an electron mediator in anaerobic respiration by the NADH-fumarate reductase system of other eukaryotes. This also suggests that the mitochondria of *E. multilocularis* protoscoleces possess an anaerobic respiratory chain in which complex II of the parasite functions as a rhodoquinol-fumarate reductase. Furthermore, in vitro treatment assays using respiratory chain inhibitors against the NADH-quinone reductase activity of mitochondrial complex I demonstrated that they had a potent ability to kill protoscoleces. These results suggest that the mitochondrial respiratory chain of the parasite is a promising target for chemotherapy of alveolar echinococcosis.

Echinococcosis is a near-cosmopolitan zoonosis caused by helminthic parasites belonging to the genus *Echinococcus* (family Taeniidae) (18). The life cycle of *Echinococcus* spp. includes an egg-producing adult stage in the definitive hosts and a larval stage in intermediate hosts including humans. The larval stage of the parasite produces a large number of infective protoscoleces that develop to adult worms after being ingested by the definitive host, or they produce a new parasite mass when liberated inside the intermediate host, causing metastases of the parasite lesions. The two major species of medical and public health importance are *Echinococcus granulosus* and *E. multilocularis*, which cause cystic echinococcosis and alveolar echinococcosis (AE), respectively.

Human AE is a life-threatening disease, and without careful clinical management, it has a high fatality rate and poor prognosis. Humans acquire AE infection by ingesting eggs from adult parasitic worms. Early diagnosis and treatment (mainly by radical surgery) of human AE are difficult because the disease progresses slowly and usually takes more than several years before clinical symptoms become apparent. An efficient chemotherapeutic compound is still not available. The first choice for the chemotherapy of AE is benzimidazole derivatives (18), but they are parasitostatic rather than parasitocidal against larval *E. multilocularis*. Therefore, the development of highly effective antiechinococcal drugs is urgently needed.

Biological systems for energy metabolism are essential for the survival, continued growth, and reproduction of all living organisms. "Typical" mitochondria are usually considered to be oxygen-consuming, ATP-producing organelles. In fact, typical mitochondria, such as those found in mammalian cells, require oxygen to function. They use pyruvate dehydrogenase for oxidative decarboxylation of pyruvate to acetyl coenzyme A, which is then completely oxidized to CO_2 through the Krebs cycle. Most of the energy is produced by oxidative phosphorylation: the electrons from NADH and succinate are transferred to oxygen by the proton-pumping electron transfer respiratory chain in which ubiquinone (UQ) (Fig. 1A) is commonly used as an electron mediator. The backflow of the protons results in ATP formation by the mitochondrial ATP synthase.

In parasitic organisms, on the other hand, the carbohydrate and energy metabolic pathways of adult parasitic helminths differ greatly from those of their vertebrate hosts. The most important factors in this respect are the nutrient and oxygen supply (reviewed in references 4, 12, and 13). Parasitic hel-

* Corresponding author. Mailing address: Department of Biomedical Chemistry, Graduate School of Medicine, University of Tokyo, Tokyo 113-0033, Japan. Phone: 81 3 58418202. Fax: 81 3 58413444. E-mail: sakamok@m.u-tokyo.ac.jp.

▽ Published ahead of print on 22 October 2007.

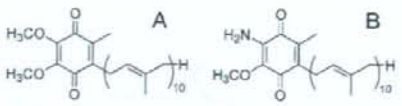

FIG. 1. Chemical structure of ubiquinone-10 (UQ_{10}) (E_m' = +110 mV) (A) and rhodoquinone-10 (RQ_{10}) (E_m' = −63 mV) (B).

minths have exploited a variety of energy-transducing systems during their adaptation to habitats in their hosts (7, 28). The parasitic nematode *Ascaris suum*, for example, resides in the host small intestine, where oxygen tensions are low, and exploits a unique anaerobic respiratory chain, called the NADH-fumarate reductase system, to adapt to its microaerobic habitat (Fig. 2) (2, 3, 14, 22; reviewed in reference 10). The NADH-fumarate reductase system is part of the unique respiratory system for parasitic helminthes and is the terminal step in the phosphoenolpyruvate carboxykinase-succinate pathway, which is found in many anaerobic organisms. Electrons from NADH are accepted by rhodoquinone (RQ) (Fig. 1B) via the NADH-RQ reductase activity of mitochondrial complex I and then transferred to fumarate through the rhodoquinol-fumarate reductase activity of mitochondrial complex II. The anaerobic electron transfer in complex I couples with proton transport across the mitochondrial inner membrane, providing ATP even in the absence of oxygen. This system, which does not normally function in mammalian mitochondria, is considered to be a good target for the development of novel anthelminthics (8, 9, 21). With regard to *Echinococcus* spp., the presence of both aerobic and anaerobic respiratory systems was previously suggested by a series of intensive studies (1, 16, 17), although the respiratory systems in this group of parasites are to be characterized in more detail.

In the present study, we prepared an enriched mitochondrial fraction from *E. multilocularis* protoscoleces and characterized the specific enzyme activities involved in mitochondrial energy metabolism as well as the quinone profile in the parasite's respiratory chain. Furthermore, based on findings reported previously by Yamashita et al. that quinazoline derivatives can inhibit the NADH-quinone reductase of mitochondria from *A. suum* (35), we tested several quinazoline-type compounds, with a view to developing novel antiechinococcal compounds.

MATERIALS AND METHODS

Isolation of *E. multilocularis* protoscoleces. We used the Nemuro strain of *E. multilocularis*, which is maintained at the Hokkaido Institute of Public Health (Sapporo, Japan). Mature larval parasites with protoscolex formation were obtained from cotton rats (*Sigmodon hispidus*) more than 4 months after oral infection with 50 parasite eggs. To isolate protoscoleces, the mature larval parasites were minced with scissors, pushed through a metal mesh, and washed repeatedly with physiological saline until host materials were thoroughly removed.

Preparation of enriched mitochondrial fractions. The enriched mitochondrial fractions of *E. multilocularis* protoscoleces were prepared essentially according to methods described previously for isolating adult *Ascaris* mitochondria (25, 26). Briefly, the isolated protoscolex sediment was suspended in 5 volumes of mitochondrial preparation buffer (210 mM mannitol, 10 mM sucrose, 1 mM disodium EDTA, and 50 mM Tris-HCl [pH 7.5]) supplemented with 10 mM sodium malonate. The parasite materials were homogenized with a motor-driven glass/glass homogenizer (six passes three to four times). The homogenate was diluted with the mitochondrial preparation buffer to 10 times the volume of the original protoscolex sediment and then centrifuged at 800 × *g* for 10 min to precipitate cell debris and nuclei. The supernatant was then centrifuged at 8,000 × *g* for 10 min to obtain the mitochondrial pellet. The pellet was resuspended in mitochondrial preparation buffer (without malonate) and centrifuged at 12,000 × *g* for 10 min. The resulting enriched mitochondrial fraction was suspended in mitochondrial preparation buffer (without malonate). The protein concentration was determined according to the method of Lowry et al. by using bovine serum albumin as a standard (15).

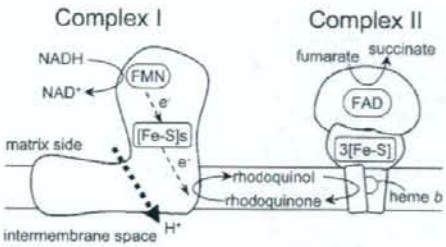

FIG. 2. Schematic representation of the NADH-fumarate reductase system in adult *A. suum*, which catalyzes the final step of the phosphoenolpyruvate carboxykinase-succinate pathway. In this system, the reducing equivalent of NADH is transferred to the low-potential RQ by the NADH-RQ reductase activity of mitochondrial complex I. This pathway ends with the production of succinate by the rhodoquinol-fumarate reductase activity of complex II. Electron transfer from NADH to fumarate is coupled to the site I phosphorylation of complex I via the generation of a proton-motive force. FMN, flavin mononucleotide; FAD, flavin adenine dinucleotide; [Fe-S]s and 3[Fe-S], iron-sulfur clusters.

Western blotting. An enriched mitochondrial fraction prepared from *E. multilocularis* protoscoleces and that from the liver of a cotton rat (used as the host animal for the parasite) were analyzed by Western blotting. Reactions were performed according to a method described previously by Towbin et al. (30). The proteins were separated by sodium dodecyl sulfate-polyacrylamide gel electrophoresis on a 10% or 15% acrylamide gel and electrophoretically transferred onto a nitrocellulose membrane. The membrane was soaked in 1:5,000 anti-cytochrome *c* oxidase subunit IV antibody (component of the ApoAlert cell fractionation kit; Clontech Laboratories) in phosphate-buffered saline containing 0.05% (wt/vol) Tween 20 and 2% (wt/vol) skim milk. The membrane was incubated for 60 min at room temperature and then washed three times for 10 min with washing buffer, which consisted of 0.05% (wt/vol) Tween 20 in phosphate-buffered saline. Alkaline phosphatase-conjugated goat anti-mouse immunoglobulin G was then added as a secondary antibody, and the mixture was incubated for 30 min. After another wash with washing buffer, the membrane was soaked in reaction buffer (100 mM Tris-HCl [pH 9.5], 100 mM NaCl, 5 mM $MgCl_2$, 500 μg/ml of 4-nitroblue tetrazolium chloride, and 165 μg/ml of 5-bromo-4-chloro-3-indolylphosphate) to initiate the development of a colored product. Finally, the membrane was washed with distilled water to stop the reaction. For Western blotting, the amounts of parasite and cotton rat mitochondrial samples were normalized by the total protein amount or cytochrome *c* oxidase activity (see below).

Enzyme assays. All enzyme assays using the enriched mitochondrial fractions were performed in a 0.7- or 1-ml reaction mixture at 25°C. The reagents used in each assay were mixed with reaction buffer containing 30 mM potassium phosphate (pH 7.4) and 1 mM $MgCl_2$. The final mitochondrial protein concentration was 80 μg per ml of reaction mixture. For all reactions performed under anaerobic conditions, the reaction medium was supplemented with 100 μg/ml glucose oxidase, 2 μg/ml catalase, and 10 mM β-D-glucose and left for 3 min to achieve anaerobiosis. NADH oxidase activity in the isolated mitochondrial fraction was determined in the presence or absence of 2 mM KCN, 100 mM malonate, or both by measuring the absorbance of NADH at 340 nm (ε = 6.2 mM^{-1} cm^{-1}). The reaction was initiated by the addition of 100 μM of NADH to the mixture. Succinate dehydrogenase (SDH) activity was determined by monitoring the absorbance change of 2-(4,5-dimethyl-2-thiazolyl)-3,5-diphenyl-2*H*-tetrazolium bromide (MTT; 60 μg/ml) at 570 nm in the presence of 120 μg/ml phenazine methosulfate and 2 mM KCN. The reaction was initiated by the addition 10 mM of succinate to the mixture. Succinate-quinone reductase activity was assayed under aerobic or anaerobic conditions in the presence of 0.1%(wt/vol) sucrose monolaurate by determining the amount of decyl UQ (dUQ) or decyl RQ (dRQ)

from the absorbance change at 278 nm (ε = 12.7 mM^{-1} cm^{-1}) or 287 nm (ε = 9.2 mM^{-1} cm^{-1}), respectively. Decyl rhodoquinol-fumarate reductase activity was measured under anaerobic conditions in a reaction mixture containing 0.1% (wt/vol) sucrose monolaurate. In this reaction, 60 μM dRQ was reduced to decyl rhodoquinol in the cuvette by adding 200 μM $NaBH_4$. The reaction was started by adding 5 mM fumarate to the mixture, and the oxidation of decyl rhodoquinol was monitored at 287 nm. NADH-fumarate reductase activity was determined by monitoring the oxidation of NADH (100 μM) at 340 nm under anaerobic conditions. The reaction was initiated by the addition of 5 mM fumarate as an electron acceptor. NADH-quinone reductase activity assays were carried out under anaerobic conditions using the same reaction mixture as that used for the NADH-fumarate reductase activity assay except that 60 μM dUQ or dRQ was used as an electron acceptor instead of fumarate. The enzyme activity was determined by monitoring the absorbance change of NADH at 340 nm. Ubiquinol oxidase activity was determined by monitoring the absorbance change of ubiquinol-1 (150 μM) at 278 nm (ε = 12.7 mM^{-1} cm^{-1}) in the presence or absence of 2 mM KCN. The activity of cytochrome *c* oxidase was determined as *N,N,N',N'*-tetramethyl-*p*-phenylenediamine dihydrochloride (TMPD) oxidase activity, which was measured by monitoring the absorbance change of TMPD (500 μM) at 610 nm (ε = 11.0 mM^{-1} cm^{-1}) in the presence or absence of 2 mM KCN.

Enzyme inhibition assays. Based on the findings of Yamashita et al. showing that that quinazoline-type compounds inhibit the NADH-quinone reductase activity of *A. suum* complex I (35), we determined 50% inhibitory concentration (IC_{50}) values of the quionazoline-type compounds against NADH-fumarate reductase activity of the parasite mitochondria and the NADH oxidase activity of bovine heart mitochondria (see "Enzyme assays"). The compounds used in the assays included quinazoline and its derivatives 6-NH_2, 6-$NHCO(CH{=}CH_2)$, 7-NH_2, 8-OH, 8-OCH_3, 8-OCH_2CH_3, and 8-$OCH(CH_3)_2$.

Analysis of the quinone profile of isolated mitochondria. Quinones were extracted from lyophilized mitochondria essentially according to a method described previously by Takada et al. (24). A lyophilized mitochondrial sample (2.9 mg protein) was crushed into powder before extraction, vortexed in 2:5 (vol/vol) ethanol/*n*-hexane for 10 min, and centrifuged at 20,000 × *g* for 5 min at room temperature. The supernatants were pooled, and the extraction of quinones was repeated twice. Pooled extracts were evaporated to dryness, dissolved in ethanol, and kept in the dark until high-performance liquid chromatography (HPLC) analysis. Quinones were applied to a reverse-phase HPLC column (Inertsil ODS-3 [5 μm and 4.6 by 250 mm]; GL Science) and eluted under isocratic conditions (1 ml/min) with 1:4 (vol/vol) diisopropyl ether-methanol at 25°C. The molecular species of the eluted quinones were identified by their retention times and by their spectral characteristics as measured with a UV-visible photodiode array (Shimadzu SPD-10-A). The concentration of quinones was determined spectrophotometrically. The major quinone detected was confirmed by mass spectrometry (MS) using an Applied Biosystems API-165 LC/MS system with electrospray ionization.

In vitro treatment of *E. multilocularis* protoscoleces. *E. multilocularis* protoscoleces were obtained as described above (see "Isolation of *E. multilocularis* protoscoleces"). The parasite materials were placed into culture medium suitable for the long-term maintenance of the protoscoleces in vitro (27). The parasite cultures were kept in a six-well plate at a density of approximately 500 protoscoleces per ml of culture medium, and half of the medium was replaced twice a week. This culture condition was also applied during in vitro treatment of the parasite. To examine the efficacy of chemical compounds against living *E. multilocularis* protoscoleces, the parasites were kept in the culture medium supplemented with 5 or 50 μM of each compound, including quinazoline and its 8-OH derivative, rotenone (a specific inhibitor of mitochondrial complex I) (19) and nitazoxanide (a compound with strong protoscolicidal action) (32). One control group was supplemented with 0.5% (vol/vol) dimethyl sulfoxide (vehicle) alone, and all conditions were assayed in triplicate. The viability of protoscoleces was determined by microscopic analysis of more than 170 protoscoleces per well for motile behavior and the ability to exclude trypan blue (32).

RESULTS

Preparation of enriched mitochondrial fractions. To characterize the mitochondrial respiratory chain of *E. multilocularis* protoscoleces, we prepared enriched mitochondrial fractions from the parasite. Approximately 80 g of larval *E. multilocularis* (containing approximately 10^5 protoscoleces per gram) was obtained from each cotton rat more than 4 months after oral infection with 50 parasite eggs. Approximately 20 g of the larval parasite was used per isolation of protoscoleces, yielding 2 ml of cleaned protoscolex sediment (Fig. 3). The enriched mitochondrial fractions were prepared from the protoscolex sediment as described in Materials and Methods. Each 1 ml of protoscolex sediment (containing 4.5 × 10^5 protoscoleces) yielded approximately 4 mg of mitochondria. Western blotting using an antibody to mammalian cytochrome *c* oxidase detected a specific band in the mitochondria from the liver of a cotton rat but not in mitochondria from *E. multilocularis* protoscoleces even when the amounts of both mitochondrial samples were normalized according to cytochrome *c* oxidase activity (data not shown). These results demonstrated that the enriched mitochondrial fractions from the parasite were sufficiently free of host components for use in enzyme assays and quinone analyses. In order to assess the quality of mitochondria, intactness was examined by the reactivity of NADH, which is a non-membrane-permeable substrate. NADH oxidase activity was not detected in the isotonic buffer, whereas it was fully activated in hypotonic buffer after a freeze-thaw treatment of the enriched mitochondrial fraction. Based on the results obtained, the method applied here for mitochondrial preparation seemed to be appropriate.

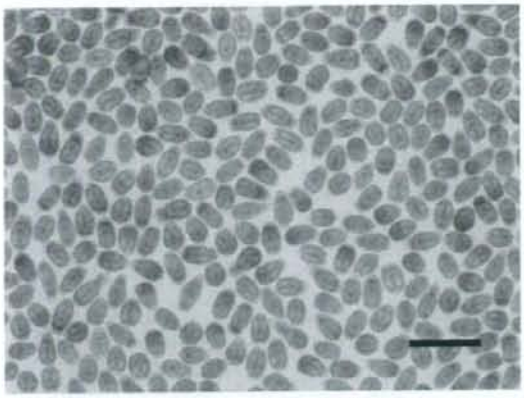

FIG. 3. Protoscoleces of *E. multilocularis* (Nemuro strain) used for the preparation of enriched mitochondrial fractions of the parasite and subsequent analyses. Bar, 500 μm.

Enzyme activities of *E. multilocularis* mitochondria. The specific enzyme activities involved in the mitochondrial respiratory chain of *E. multilocularis* protoscoleces are shown in Table 1. Parasite complex II exhibited an SDH activity of 103 nmol/min/mg. The specific activity of succinate-dUQ reductase was comparable to that of SDH activity (98.9 nmol/min/mg), whereas the succinate-dRQ reductase activity was lower (16.6 nmol/min/mg). The specific activity of decyl rhodoquinol-fumarate reductase, which is the reverse reaction of the succinate-RQ reductase activity of complex II, was determined to be 60.2 nmol/min/mg. The mitochondria of *E. multilocularis* protoscoleces exhibited NADH oxidase activity of 9.1 nmol/min/mg, which was almost eliminated by 2 mM KCN and 100 mM malonate. Ubiquinol-1 oxidase and TMPD oxidase activities were determined to be 4.4 nmol/min/mg and 12.6 nmol/

TABLE 1. Specific activities of mitochondrial respiratory enzymes in *E. multilocularis* protoscoleces

Assay	Sp act[a] (nmol/min/mg of protein) (mean ± SD)
SDH	103 ± 16
Succinate-quinone reductase	
dUQ (anaerobic)	98.9 ± 12
dRQ (anaerobic)	16.6 ± 3.5
Quinol-fumarate reductase (decyl rhodoquinol) (anaerobic)	60.2 ± 18
NADH oxidase	9.1 ± 2.1
NADH oxidase with:	
2 mM KCN	7.3 ± 1.5
100 mM malonate	4.4 ± 0.4
2 mM KCN and 100 mM malonate	1.7 ± 0.7
Ubiquinol-1 oxidase	4.4 ± 0.6
TMPD oxidase	12.6 ± 6.3
NADH-fumarate reductase (anaerobic)	45.0 ± 8.1
NADH-quinone reductase	
dUQ (anaerobic)	32.1 ± 2.7
dRQ (anaerobic)	61.3 ± 4.3

[a] Specific activities were obtained from at least three independently isolated mitochondria.

min/mg, respectively. These activities were completely inhibited by 2 mM KCN. Under anaerobic conditions, the specific activity of NADH-fumarate reductase was 45 nmol/min/mg, which was much higher than the NADH oxidase activity. The specific activity of NADH-dUQ reductase and NADH-dRQ reductase of complex I were determined to be 32.1 and 61.3 nmol/min/mg, respectively.

Quinone components in *E. multilocularis* mitochondria. To determine which quinones act as physiological electron mediators in the mitochondrial respiratory system of *E. multilocularis* protoscoleces, HPLC analyses were performed. As shown in Fig. 4A, the enriched mitochondrial fractions contained only one major quinone component at a retention time (*Rt*) of 22.4 min. The peak fraction exhibited a characteristic absorption maximum for RQs at 283 nm (Fig. 4B) (20). Subsequent MS analysis confirmed that the primary quinone of the parasite was RQ_{10} (electrospray ionization-MS *m/z* 848.8 $[M + H]^+$). The concentration of RQ_{10} was determined to be 0.73 nmol/mg of mitochondrial protein.

Effects of inhibitors on NADH-fumarate reductase in *E. multilocularis* mitochondria. To investigate the inhibitory effect of quinazoline (Fig. 5A) and its derivatives on the enzymatic activities in the anaerobic respiratory system of *E. multilocularis* mitochondria, we determined IC_{50} values against the NADH-fumarate reductase activity of the enriched mitochondrial fraction of the parasite. We found that all of the compounds inhibited the NADH-fumarate reductase activity of the parasite to some extent. Quinazoline and its derivatives including 6-NH_2, 6-$NHCO(CH{=}CH_2)$, 7-NH_2, 8-OH, 8-OCH_3, 8-OCH_2CH_3, and 8-$OCH(CH_3)_2$ exhibited IC_{50} values of 2.3, 2.1, 16, 62, 71, 48, 4,100, and 910 nM, respectively. Of the compounds tested, the 8-OH derivative (Fig. 5B) exhibited relatively selective inhibition against the NADH-fumarate reductase activity of *E. multilocularis* protoscoleces compared with the NADH oxidase activities of mammalian mitochondria: the IC_{50} values of quinazoline and its 8-OH derivative for

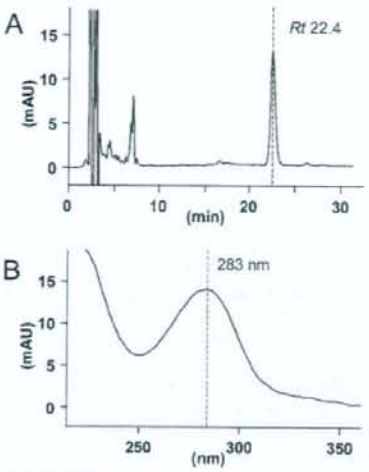

FIG. 4. (A) HPLC analysis of quinones extracted from the enriched mitochondrial fraction of *E. multilocularis* protoscoleces. Detailed experimental conditions are described in Materials and Methods. The highest peak had a retention time of 22.4 min (arrow). (B) Absorption of this peak was 283 nm, suggesting that it contained an RQ. mAU, milli-absorbance units.

the NADH oxidase activities of mammalian (bovine heart) mitochondria were 0.40 and 230 nM, respectively.

Effects of inhibitors on living *E. multilocularis* protoscoleces. In order to examine the parasite-killing activities of the quinazoline-type compounds with different degrees of inhibitory effects against NADH-fumarate activities of *E. multilocularis* protoscoleces, we performed in vitro treatment of the parasite using quinazoline and its 8-OH derivative. The viability of the *E. multilocularis* protoscolex was progressively reduced during in vitro treatment of the parasites with 50 μM of the 8-OH derivative, and by day 5, all the parasites died (Fig. 6). The same compound did not have an obvious antiparasitic effect when used at a concentration of 5 μM. On the other hand, nonsubstituted quinazoline, which showed lower IC_{50} values with the enzymatic assay, eliminated the parasites on days 5 and 7 of in vitro treatment when used at 50 and 5 μM, respectively. Treatment with rotenone, a specific inhibitor of mitochondrial complex I (19), affected the viability of the parasite in a manner similar to that of the 8-OH derivative. The anti-echinococcal effect of nitazoxanide was relatively mild: even in

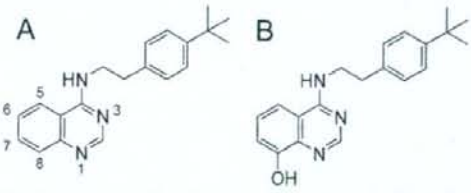

FIG. 5. Structures of quinazoline (A) and its 8-OH derivative (B) used for the enzyme inhibition assays and in vitro treatment of *E. multilocularis* protoscoleces.

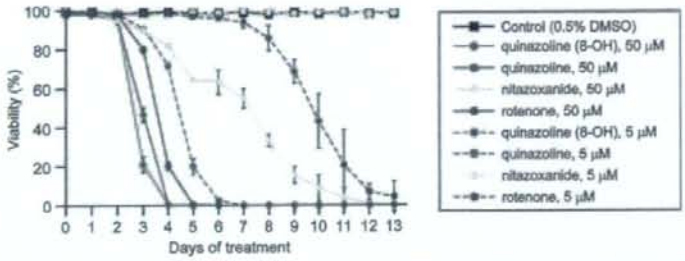

FIG. 6. Viability of *E. multilocularis* protoscoleces during in vitro treatment with quinazoline and its 8-OH derivatives, rotenone and nitazoxanide. Each compound was added to the culture medium at 5 or 50 μM. The results represent the means ± standard deviations of at least triplicate samples. DMSO, dimethyl sulfoxide.

the presence of 50 μM nitazoxanide, the viability decreased, but it did so only gradually, and it took 13 days before all the protoscoleces died. This compound did not affect parasite viability when used at 5 μM.

DISCUSSION

The most notable finding of the present study is that *E. multilocularis* protoscoleces possess a unique mitochondrial respiratory system that is highly adapted to anaerobic conditions. Specifically, the predominant enzymatic activity in the enriched mitochondrial fraction prepared from the parasite protoscoleces is the NADH-fumarate reductase system, which does not normally function in the aerobic respiratory chain of mammals. Thus, we infer that mitochondrial respiratory system of *E. multilocularis* would be a good target for the development of novel selective antiechinococcal compounds as demonstrated previously for other helminthic diseases (8, 21).

As early as 1957, Agosin found that *E. granulosus* protoscoleces have both aerobic and anaerobic respiratory systems and that glycolytic inhibitors are effective against both of them, indicating that they both depend on glycolysis (1). Subsequently, McManus and Smyth observed that protoscoleces cultured under anaerobic conditions produce more succinate than parasites kept under aerobic conditions, suggesting that the parasites survive under anaerobic conditions by utilizing the NADH-fumarate reductase system (16). Furthermore, McManus and Smyth reported that the specific activity of fumarate reductase in *Echinococcus* protoscoleces is lower than those of enzymes involved in the tricarboxylic acid cycle (17). These results, however, did not establish the importance of NADH-fumarate reductase activity in the mitochondrial respiratory system of the parasite because the other enzyme activities were not analyzed.

In the present study, we focused on the enzyme activities of the mitochondrial respiratory system of the parasite to determine whether the system is adapted to anaerobic conditions. Using the enriched mitochondrial fractions prepared from *E. multilocularis* protoscoleces, we showed that the activity of NADH-fumarate reductase in the respiratory system of the parasite is predominant compared with that of NADH oxidase, an enzyme involved in aerobic respiration in aerobic organisms such as mammals. Furthermore, direct measurements of complex II activities in both directions (i.e., succinate-RQ reductase and rhodoquinol-fumarate reductase activities) indicated that parasite complex II functions more favorably as a rhodoquinol-fumarate reductase in the presence of RQ/rhodoquinol. Thus, our results using isolated mitochondria of *E. multilocularis* protoscoleces coupled with assay systems for the determination of the parasite's enzyme activities revealed for the first time that the parasite mitochondria are highly adapted to anaerobic environments.

Analyses of the quinone components of *E. multilocularis* mitochondria revealed that RQ_{10} (Fig. 1B), whose redox potential is much more negative (E_m' [midpoint potential] = −63 mV) than that of UQ_{10} (E_m' = +110 mV) (Fig. 1A), was the primary quinone component of parasite mitochondria. In other parasitic helminths, like *A. suum* and *Hymenolepis diminuta*, RQ is an essential component of the NADH-fumarate reductase system (5, 11). In addition, van Hellemond et al. previously demonstrated that for all eukaryotes, the relative amount of RQ compared to the total amount of quinones correlates well with the importance of fumarate reduction in vivo (31). Similarly, during the development of the liver fluke *Fasciola hepatica*, there is a good correlation between the quinone composition and the importance of fumarate reduction in vivo (31). Therefore, RQ seems to be an essential component of fumarate reduction in eukaryotic respiration. Although menaquinone-related fumarate reduction in prokaryotes is well known (33, 34), there is no evidence that menaquinone serves this function in eukaryotes. In this study, enzyme assays demonstrated that the mitochondria from *E. multilocularis* possess NADH-fumarate activity as the predominant activity. In addition, the NADH-dRQ reductase activity was much higher than that of NADH-dUQ reductase, indicating that *E. multilocularis* complex I may interact preferentially with RQ rather than with UQ. Taken together, these results indicate that, as in other metazoan eukaryotes with anaerobic respiratory systems, *E. multilocularis* protoscoleces have a unique respiratory system that is highly adapted to anaerobic environments and in which RQ_{10} is used as the primary electron mediator.

Spiliotis et al. recently reported that the in vitro growth of larval *E. multilocularis* is more active under anaerobic than aerobic conditions (23). Thus, our findings for the respiratory system of *E. multilocularis* protoscoleces are consistent with the observations reported previously by Spiliotis et al. Larval *E. multilocularis* containing a large number of protoscoleces

lives in host tissues, mainly the liver, surrounded by thick connective tissues containing carbohydrate-rich laminated layers, which probably provide the parasite cells with an extremely-low-oxygen environment. Accordingly, it is not surprising that the parasite survives in the host by utilizing an anaerobic respiratory system.

Many anaerobic parasitic eukaryotes use the NADH-fumarate pathway, which is absent in mammals (2, 3, 10, 14, 22, 29). Therefore, this unique respiratory system is regarded as a promising chemotherapeutic target for the development of novel anthelminthics, as discussed in a recent review (9). In fact, Omura et al. previously found a natural compound, nafuredin, that is a potent inhibitor of the adult *A. suum* mitochondrial respiratory chain but much weaker against the mammalian mitochondrial respiratory chain (21). Yamashita et al. also found that quinazoline-type inhibitors were highly effective against adult *A. suum* complex I (35). Kinetic analyses using a series of quinazoline-type inhibitors revealed that *A. suum* complex I recognizes RQ_2 or UQ_2 in different ways, suggesting that mitochondrial complex I, which reacts preferably with RQs, could be a good target for chemotherapy. In the present study, we also tested several quinazoline-type compounds for their abilities to inhibit the anaerobic respiratory system of *E. multilocularis* protoscoleces. We found that all of the quinazoline-type compounds inhibited the NADH-fumarate reductase activity of *E. multilocularis* mitochondria to different extents. Furthermore, these compounds exhibited potent parasite-killing activities against *E. multilocularis* protoscoleces under in vitro culture conditions. Importantly, the nonsubstituted quinazoline, which has a higher inhibitory effect against NADH-fumarate oxidoreductase of the parasite mitochondria than the 8-OH derivative does, exhibited the parasite-killing activity even when used at 5 μM, whereas the 8-OH derivative did not do so at the same concentration. Such a correlation between the enzyme inhibition and the parasite-killing activities of these compounds suggests that the anaerobic NADH-fumarate reductase system of the parasite is a promising target for the development of antiechinococcal drugs.

Antiechinococcal drugs for chemotherapy of human AE should target not only protoscoleces but also the germinal layers of the *E. multilocularis* metacestode. The germinal layers in the larval parasite exhibit extremely unique characteristics. The parasite cells forming the germinal layers can differentiate into various tissues, including brood capsules and protoscoleces, and at the same time, they proliferate asexually as they remain in an undifferentiated state. This causes enlargement and, occasionally, metastasis of the lesions due to the formation of a large parasite mass. Therefore, for chemotherapy of AE, a complete cure cannot be achieved unless the germinal cells of the larval parasite are eliminated. Therefore, the mitochondrial respiratory system of germinal cells should be further characterized to aid in the development of a novel antiechinococcal compound(s) targeting the energy metabolism of larval *E. multilocularis*. However, it is presently quite difficult to obtain enough metacetode materials with homogeneous quality. Established methodologies for the in vitro cultivation of *E. multilocularis* metacestodes are now available (6, 23), and they will hopefully be applicable to large-scale preparations of metacestode materials in the near future.

During the life cycle of *E. multilocularis*, the parasite never undergoes active development and/or energy metabolism under aerobic conditions. The larval parasite lives mainly in the liver of intermediate host animals, whereas the adult worm dwells inside the small intestine of the final host, both of which are microaerobic conditions. Although the eggs of the parasite are exposed to air, they already contain a mature infective larva (oncosphere) waiting to be taken up by the next intermediate host. Therefore, the oncosphere does not develop or move under aerobic conditions. Taken together, these findings suggest that the respiratory system of *E. multilocularis* protoscoleces, as characterized in the present study, could represent the respiratory system used by the parasite throughout its developmental stages. Based on this speculation, the use of protoscolex materials in the first-step screening of candidate compounds by enzyme inhibition assays and subsequent in vitro parasite-killing assays appears to be reasonable, although it should be confirmed that the respiratory system of the *E. multilocularis* metacestode shares the same basic characteristics with that of the protoscolex stage of the parasite. We have already done preliminary experiments on the effects of the compounds used in this study, including the quinazoline derivative (8-OH), against in vitro-cultured metacestodes and found that the compounds exhibited high parasite-killing activities as evaluated by a modified MTT assay (data not shown). These results strongly suggest that our strategy is appropriate.

Highly effective chemotherapeutic compounds against human AE are not currently available despite the fact that the disease can be lethal unless the patient is appropriately treated during the early stage of the infection. Based on the findings presented here, it appears that the anaerobic respiratory system of *E. multilocularis*, which is distinct from that of host mammals, is a good target for the development of highly effective antiechinococcal drugs and, furthermore, that respiratory chain inhibitors (21, 35) are possible lead compounds for the development of antiechinococcal drugs.

ACKNOWLEDGMENTS

We thank Andrew Hemphill at the University of Berne for kindly providing us with precious chemical compounds.

This work was supported by grants from the following organizations: the Ministry of Education, Culture, Sports, Science, and Technology of Japan for the 21st Century COE Program, Program of Excellence for Zoonosis Control, and 18073004; the Ministry of Health and Welfare, Japan, for the Control of Emerging and Reemerging Diseases in Japan; the Japan Society of the Promotion of Science (grants 17790274 and 18GS0314); the Northern Advancement Center for Science and Technology; and the Akiyama Foundation.

REFERENCES

1. **Agosin, M.** 1957. Studies on the metabolism of *Echinococcus granulosus*. II. Some observations on the carbohydrate metabolism of hydatid cyst scolices. Exp. Parasitol. **6**:586–593.
2. **Amino, H., A. Osanai, H. Miyadera, N. Shinjyo, T. Tomitsuka, H. Taka, R. Mineki, K. Murayama, S. Takamiya, T. Aoki, H. Miyoshi, K. Sakamoto, S. Kojima, and K. Kita.** 2003. Isolation and characterization of the stage-specific cytochrome *b* small subunit (CybS) of *Ascaris suum* complex II from the aerobic respiratory chain of larval mitochondria. Mol. Biochem. Parasitol. **128**:175–186.
3. **Amino, H., H. Wang, H. Hirawake, F. Saruta, D. Mizuchi, R. Mineki, N. Shindo, K. Murayama, S. Takamiya, T. Aoki, S. Kojima, and K. Kita.** 2000. Stage-specific isoforms of *Ascaris suum* complex. II. The fumarate reductase of the parasitic adult and the succinate dehydrogenase of free-living larvae share a common iron-sulfur subunit. Mol. Biochem. Parasitol. **106**:63–76.
4. **Bryant, C., and C. Behm.** 1989. Energy metabolism, p. 25–69. *In* C. Bryant

and C. Behm (ed.), Biochemical adaptation in parasites. Chapman and Hall, London, United Kingdom.
5. **Fioravanti, C. F., and Y. Kim.** 1988. Rhodoquinone requirement of the *Hymenolepis diminuta* mitochondrial electron transport system. Mol. Biochem. Parasitol. **28:**129–134.
6. **Hemphill, A., and B. Gottstein.** 1995. Immunology and morphology studies on the proliferation of in vitro cultivated *Echinococcus multilocularis* metacestodes. Parasitol. Res. **81:**605–614.
7. **Kita, K., H. Hirawake, and S. Takamiya.** 1997. Cytochromes in the respiratory chain of helminth mitochondria. Int. J. Parasitol. **27:**617–630.
8. **Kita, K., C. Nihei, and E. Tomitsuka.** 2003. Parasite mitochondria as drug target: diversity and dynamic changes during the life cycle. Curr. Med. Chem. **10:**2535–2548.
9. **Kita, K., K. Shiomi, and S. Omura.** 2007. Advances in drug discovery and biochemical studies. Trends Parasitol. **23:**223–229.
10. **Kita, K., and S. Takamiya.** 2002. Electron-transfer complexes in *Ascaris* mitochondria. Adv. Parasitol. **51:**95–131.
11. **Kita, K., S. Takamiya, R. Furushima, Y. Ma, H. Suzuki, T. Ozawa, and H. Oya.** 1988. Electron-transfer complexes of *Ascaris suum* muscle mitochondria. III. Composition and fumarate reductase activity of complex II. Biochim. Biophys. Acta **935:**130–140.
12. **Köhler, P.** 1991. The pathways of energy generation in filarial parasites. Parasitol. Today **7:**21–25.
13. **Komuniecki, R., and B. G. Harris.** 1995. Carbohydrate and energy metabolism in helminths, p. 49–66. *In* J. J. Marr and M. Müller (ed.), Biochemistry and molecular biology of parasites. Academic Press, New York, NY.
14. **Kuramochi, T., H. Hirawake, S. Kojima, S. Takamiya, R. Furushima, T. Aoki, R. Komuniecki, and K. Kita.** 1994. Sequence comparison between the flavoprotein subunit of the fumarate reductase (complex II) of the anaerobic parasitic nematode, *Ascaris suum* and the succinate dehydrogenase of the aerobic, free-living nematode, *Caenorhabditis elegans*. Mol. Biochem. Parasitol. **68:**177–187.
15. **Lowry, O. H., N. J. Rosebrough, A. L. Farr, and R. J. Randall.** 1951. Protein measurement with the Folin phenol reagent. J. Biol. Chem. **193:**265–275.
16. **McManus, D. P., and J. D. Smyth.** 1978. Differences in the chemical composition and carbohydrate metabolism of *Echinococcus granulosus* (horse and sheep strains) and *E. multilocularis*. Parasitology **77:**103–109.
17. **McManus, D. P., and J. D. Smyth.** 1982. Intermediary carbohydrate metabolism in protoscoleces of *Echinococcus granulosus* (horse and sheep strains) and *E. multilocularis*. Parasitology **84:**351–366.
18. **McManus, D. P., W. Zhang, J. Li, and P. B. Bartley.** 2003. Echinococcosis. Lancet **362:**1295–1304.
19. **Miyoshi, H.** 1998. Structure-activity relationships of some complex I inhibitors. Biochim. Biophys. Acta **1364:**236–244.
20. **Moore, H. W., and K. Folkers.** 1965. Coenzyme Q. LXII. Structure and synthesis of rhodoquinone, a natural aminoquinone of the coenzyme Q group. J. Am. Chem. Soc. **87:**1409–1410.
21. **Omura, S., H. Miyadera, H. Ui, K. Shiomi, Y. Yamaguchi, R. Masuma, T. Nagamitsu, D. Takano, T. Sunazuka, A. Harder, H. Kölbl, M. Namikoshi, H. Miyoshi, K. Sakamoto, and K. Kita.** 2001. An anthelmintic compound, nafuredin, shows selective inhibition of complex I in helminth mitochondria. Proc. Natl. Acad. Sci. USA **98:**60–62.
22. **Saruta, F., T. Kuramochi, K. Nakamura, S. Takamiya, Y. Yu, T. Aoki, K. Sekimizu, S. Kojima, and K. Kita.** 1995. Stage-specific isoforms of complex II (succinate-ubiquinone oxidoreductase) in mitochondria from the parasitic nematode, *Ascaris suum*. J. Biol. Chem. **270:**928–932.
23. **Spiliotis, M., D. Tappe, L. Sesterhenn, and K. Brehm.** 2004. Long-term in vitro cultivation of *Echinococcus multilocularis* metacestodes under axenic conditions. Parasitol. Res. **92:**430–432.
24. **Takada, M., S. Ikenoya, T. Yuzuriha, and K. Katayama.** 1982. Studies on reduced and oxidized coenzyme Q (ubiquinones). II. The determination of oxidation-reduction levels of coenzyme Q in mitochondria, microsomes and plasma by high-performance liquid chromatography. Biochim. Biophys. Acta **679:**308–314.
25. **Takamiya, S., R. Furushima, and H. Oya.** 1984. Electron transfer complexes of *Ascaris suum* muscle mitochondria. I. Characterization of NADH-cytochrome *c* reductase (complex I-III), with special reference to cytochrome localization. Mol. Biochem. Parasitol. **13:**121–134.
26. **Takamiya, S., K. Kita, H. Wang, P. P. Weinstein, A. Hiraishi, H. Oya, and T. Aoki.** 1993. Developmental changes in the respiratory chain of *Ascaris* mitochondria. Biochim. Biophys. Acta **1141:**65–74.
27. **Thompson, R. C., P. Deplazes, and J. Eckert.** 1990. Uniform strobilar development of *Echinococcus multilocularis* in vitro from protoscolex to immature stages. J. Parasitol. **76:**240–247.
28. **Tielens, A. G. M., C. Rotte, J. J. van Hellemond, and W. Martin.** 2002. Mitochondria as we don't know them. Trends Biochem. Sci. **27:**564–572.
29. **Tielens, A. G. M., and J. J. van Hellemond.** 1998. The electron transport chain in anaerobically functioning eukaryotes. Biochim. Biophys. Acta **1365:** 71–78.
30. **Towbin, H., T. Staehelin, and J. Gordon.** 1979. Electrophoretic transfer of proteins from polyacrylamide gels to nitrocellulose sheets: procedure and some applications. Proc. Natl. Acad. Sci. USA **76:**4350–4354.
31. **van Hellemond, J. J., M. Klockiewicz, C. P. Gaasenbeek, M. H. Roos, and A. G. M. Tielens.** 1995. Rhodoquinone and complex II of the electron transport chain in anaerobically functioning eukaryotes. J. Biol. Chem. **270:** 31065–31070.
32. **Walker, M., J. F. Rossignol, P. Torgerson, and A. Hemphill.** 2004. In vitro effects of nitazoxanide on *Echinococcus granulosus* protoscoleces and metacestodes. J. Antimicrob. Chemother. **54:**609–616.
33. **Wissenbach, U., A. Kroger, and G. Unden.** 1990. The specific functions of menaquinone and demethylmenaquinone in anaerobic respiration with fumarate, dimethylsulfoxide, trimethylamine *N*-oxide and nitrate by *Escherichia coli*. Arch. Microbiol. **154:**60–66.
34. **Wissenbach, U., D. Ternes, and G. Unden.** 1992. An *Escherichia coli* mutant containing only demethylmenaquinone, but no menaquinone: effects on fumarate, dimethylsulfoxide, trimethylamine *N*-oxide and nitrate respiration. Arch. Microbiol. **158:**68–73.
35. **Yamashita, T., T. Ino, H. Miyoshi, K. Sakamoto, A. Osanai, E. Nakamaru-Ogiso, and K. Kita.** 2004. Rhodoquinone reaction site of mitochondrial complex I, in parasitic helminth, *Ascaris suum*. Biochim. Biophys. Acta **1608:** 97–103.

Available online at www.sciencedirect.com
ScienceDirect
Parasitology International 57 (2008) 229–232
www.elsevier.com/locate/parint

Short communication

Mutation underlying resistance of *Plasmodium berghei* to atovaquone in the quinone binding domain 2 (Qo_2) of the cytochrome *b* gene

Josephine E. Siregar [a,d], Din Syafruddin [a,b], Hiroyuki Matsuoka [c], Kiyoshi Kita [d], Sangkot Marzuki [a,*]

[a] *Eijkman Institute for Molecular Biology, Jakarta, Indonesia*
[b] *Department of Parasitology, Faculty of Medicine, Hasanuddin University, Makassar, Indonesia*
[c] *Department of Medical Zoology, Jichi Medical University, Tochigi, Japan*
[d] *Department of Biomedical Chemistry, Graduate School of Medicine, The University of Tokyo, Tokyo, Japan*

Received 7 March 2007; received in revised form 29 November 2007; accepted 1 December 2007
Available online 8 December 2007

Abstract

The anti-malarial agent atovaquone specifically targets the cytochrome bc_1 complex and inhibits the parasite respiration. Resistance to this drug, a coenzyme Q analogue, is associated with mutations in the mitochondrial cytochrome *b* gene. We previously reported atovaquone resistant mutations in *Plasmodium berghei*, in the first quinone binding domain (Qo_1) of the cytochrome *b* gene (M133I and L144S) with V284F in the sixth transmembrane domain. However, in *P. falciparum* the most common mutations are found in the Qo_2 region. To obtain a better model for biochemical and genetic studies, we have now extended our study to isolate a wider range of *P. berghei* resistant strains, in particular those in the Qo_2. Here we report four new mutations (Y268N, Y268C, L271V and K272R), all in the Qo_2 domain. Two of these mutations are convergent to codon 268 (nt802–804) drug-induced mutation in *P. falciparum*.

Keywords: *Plasmodium berghei*; Cytochrome *b* gene mutations; Atovaquone resistance

The emergence of drug-resistant strains of *Plasmodium falciparum* within the last few decades has caused major problems in malaria treatment and control in many endemic countries. New affordable drugs that target different biochemical pathways in the malaria parasite are needed. Atovaquone, a hydroxy-1,4,-naphthoquinone, is an anti-malaria that shares structural similarity with protozoan ubiquinone, a coenzyme involved in the mitochondrial electron transport [1,2]. It is effective against chloroquine-resistant strains of *P. falciparum*, and is a major component of Malarone™ (a fixed combination of atovaquone and proguanil).

This drug collapses mitochondrial membrane potential in *Plasmodium* spp [3], and is suggested to act by competitive binding with ubiquinone at the quinone binding domain of the quinol-cytochrome *c* reductase of the mitochondrial respiratory chain (bc_1 complex, also referred to as complex III). Mutations conferring atovaquone resistance were identified in the mitochondrial cytochrome *b* (*cytb*) gene of *P. berghei* [4], *P. yoelii* [5], *P. falciparum* [6], *Pneumocystis carinii* [7], and *Toxoplasma gondii* [8]. In *Plasmodium* spp, 10 mutations, M133I, L144S, I258M, F267I, Y268C/N/S, L271F/V, K272R, P275T, G280D, and V284F had been documented, mostly located in the quinone binding domain 2 (Qo_2). Significantly, mutations affecting codon 268 (nt802–804) of the *cytb* gene in the Qo_2 domain, have been reported also in *P. falciparum* isolates collected from malaria-infected individuals in Africa, associated with the use of, and in some cases with demonstrated treatment-failure against Malarone [9–11], leading to the suggestion for its use as a molecular marker for atovaquone resistance in the field isolates [12].

The two main *P. berghei* mutations reported previously [4], M133I and L144S, were all located in the quinone binding domain 1 (Qo_1); these mutations confer up to 1000-fold

* Corresponding author. Eijkman Institute for Molecular Biology, Jalan Diponegoro 69, Jakarta 10430, Indonesia. Tel.: +62 21 3917131; fax: +62 21 3147982.
E-mail address: smarzuki@eijkman.go.id (S. Marzuki).

1383-5769/$ - see front matter © 2007 Elsevier Ireland Ltd. All rights reserved.
doi:10.1016/j.parint.2007.12.002

resistance in combination with V284F in the sixth transmembrane domain, which is adjacent to Qo_2 site. To obtain a better model for the biochemical and genetic studies of mutations observed in the human *P. falciparum*, we have now extended our study to isolate a wider range of *P. berghei* resistant strains, in particular those in the Qo_2 region conferring high degrees of resistance. Here we report four new mutations, most in the Qo_2 domain, two of which are convergent to codon 268 mutations in *P. falciparum*.

P. berghei ANKA strains were inoculated intraperitoneally into 10–12 week old BALB/c mice at approx 10^7 parasitized red blood cells/mouse. At the parasitemia level of 1–5%, the *P. berghei*-infected mice were treated intraperitoneally with different doses of atovaquone, between 0.5 and 14.4 mg kg^{-1} BW as specified in Table 1, daily for three consecutive days. Parasites were then allowed to recover for 7 days in the absence of the drug, before the same daily treatment was introduced for another 3 days. This cycle of treatment was repeated until resistance was observed, as indicated by level of parasitemia which was monitored daily. The resistant parasites were then reinoculated intraperitoneally into 10–12 week old BALB/c mice to obtain enough parasites for drug resistance test (legend of Table 1) and cryofreezing. Some isolates were further cloned by serial limiting dilution and reisolation in mice. Ten isolates were obtained, PbLSJ1 to 8 derived from *P. berghei* ANKA Leiden, and PbESJ9 and 10 from *P. berghei* ANKA Edinburgh (Table 1). In addition PbSK2A1Tb was obtained by following two passages of a frozen PbSK2A1T resistant line from our previous study [4].

Table 1
Atovaquone-resistant isolates of *P. berghei*

Isolates[a]	Atovaquone challenge[b] (mg kg^{-1} BW)	Mutation	ED50[c] (mg kg^{-1} BW)	Growth rate[d] (correlation coefficient)
PbLSJ1.1	14.4	Y268N	80	0.61 (0.96)
PbLSJ2.1	14.4	Y268C	5.2	0.86 (0.84)
PbLSJ3.1	14.4	L271V+ K272R	16	1.48 (0.96)
PbESJ9	14.4	L271V+ K272R	N.D	N.D
PbESJ10	14.4	L271V+ K272R	N.D	N.D
PbSK2A1Tb	Previous study [4]	M133I+ L271V	4	1.64 (0.84)
PbLSJ6	8	Y268N	N.D	N.D
PbLSJ4	4	Y268N	N.D	N.D
PbLSJ7	4	Y268C	N.D	N.D
PbLSJ5	2	L271V+ K272R	N.D	N.D
PbLSJ8	1	L271V+ K272R	N.D	N.D
PbL	Control	Wild type	0.01	6.05 (0.93)

[a] PbLSJ1-8 refer to mutants derived from *P. berghei* ANKA Leiden, while PbESJ9-10 from *P. berghei* ANKA Edinburgh. PbSK2A1Tb appeared following two passages of a frozen PbSK2A1T resistant strain isolated in our previous study [4]; Repeated sequencing confirmed the presence of M133I and V284F in the frozen original PbSK2A1T.

[b] The concentrations of atovaquone indicated are those employed in the isolation of resistant mutants, by treating *P. berghei*-infected BALB/c mice in cycles of 3 days of treatment and 7 days of recovery as described in the text.

[c] Drug resistance test was carried out by inoculating parasite isolates intraperitoneally into the 10–12 week old BALB/c mice, and challenging the infected mice with atovaquone at daily doses ranging from 0.001 to 50 mg kg^{-1} BW. Between three and four mice were used per *P. berghei* isolate per dose of atovaquone. Growth of parasites was determined by daily monitoring of parasitemia for 4–6 days. The 50% Effective Dose (ED50) and correlation coefficient values were calculated from the growth rates of each *P. berghei* isolate during the daily treatment with atovaquone, employing the Sigmoidal Regression Wizard.

[d] Growth rate is expressed as % increase in parasitemia day^{-1}.

A region of the 6 kb mitochondrial DNA (mtDNA) of the various *P. berghei* isolates (nt3368–nt5019) was amplified and sequenced. This region spanned the entire *cytb* gene and, therefore, includes the Qo_1 and Qo_2 domains associated with atovaquone resistance mutations [4,5]. A T to A nucleotide substitution at the first base of codon 268 (nt802) was found in three isolates (PbLSJ1.1, PbLSJ4 and PbLSJ6), leading to amino acid change Y268N in the Qo_2 domain (Table 1). Two other isolates carried an A to G substitution at the second base of the same codon (nt803), leading to amino acid change Y268C (PbLSJ2.1 and PbLSJ7). The remaining five isolates were all double mutants, carrying a T to G nucleotide substitution at nt811 and an A to G at nt815, leading to L271V and K272R, respectively. PbSK2A1Tb carried the Qo_1 G to A substitution at nt399, leading to M133I, as observed in its parental PbSK2A1T line [4], and the T to G substitution at nt811 leading to L271V in the Qo_2 domain were confirmed. Interestingly, the transmembrane V284F amino acid change of the parental line PbSK2A1T [4] has apparently disappeared during the two passages in mice.

The level of resistance of four representative isolates was determined *in vivo* as described in Table 1. The ED_{50} for the parental *P. berghei* ANKA line was found to be 0.01 mg atovaquone kg^{-1} BW, PbSJ1.1 (Y268N) showed the highest degree of resistance, with an ED_{50} of 80 mg kg^{-1} BW, while those for PbSJ2 (Y268C) and PbSJ3 (L271V+K272R) were 5.2 and 16 mg kg^{-1} BW, respectively. PbSK2A1Tb that had both Qo_1 and Qo_2 mutations (M133I+L271V) showed similar order of resistance, with an ED_{50} of 4 mg kg^{-1} BW (Table 1).

All of the mutations found in the present study are located in Qo_2 (Fig. 1), the ubiquinol oxidation domain of the cytochrome *b*, where the electron transfer to the iron–sulphur protein, and the consequent charge separation, results in proton translocation. This is in contrast to results of our earlier attempt to isolate atovaquone resistance mutants of *P. berghei* [4], which had lead to mutations in the Qo_1 domain. In the earlier study mutants were isolated by the exposure of the *P. berghei in vivo* to increasing doses of atovaquone, whereas in the present study the parasite was challenged with repeated cycles of exposure and recovery of single doses of the anti-malaria drug. It is possible that the former procedure has allowed the development of perhaps weaker Qo_1 mutants. The latter is closer to the situation in clinical treatment of malaria, and it is thus of interest to observe similar Qo_2 mutations in field isolates of *P. falciparum*(Y268S, Y268N and Y268C) [6,9,11]. Further, the isolation of *P. falciparum* resistant strains *in vitro*, by the exposure of cultured parasites with step-wise increasing doses of atovaquone, resulted in combinations of Qo_1 and Qo_2

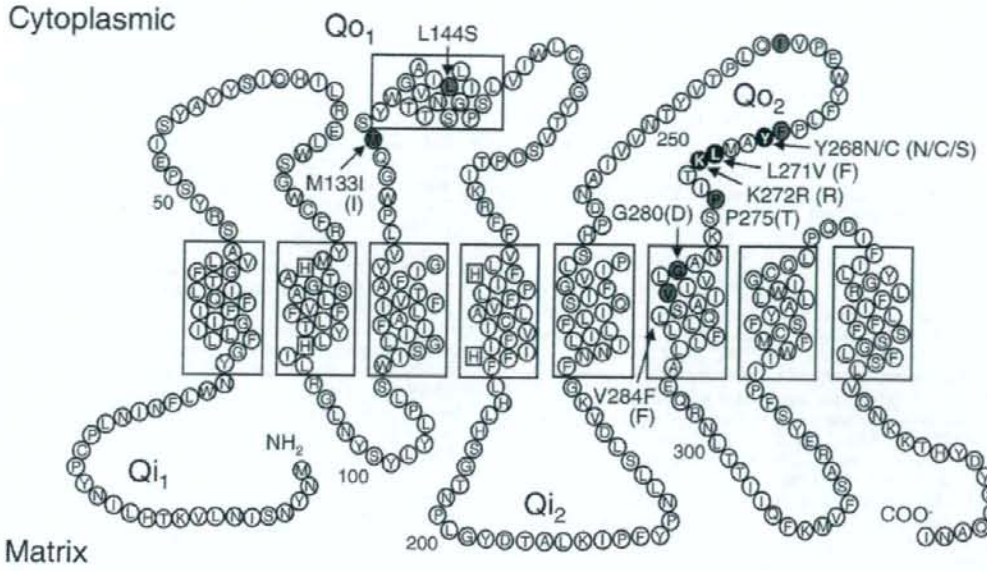

Fig. 1. Sites of atovaquone resistance mutations in the Qo_1 and Qo_2 domains of apocytochrome *b*. The apocytochrome *b* of *P. berghei* contains 376 amino acid residues and 8 transmembrane domains (boxed). Boxed "H"s are the universally conserved histidine residues that act as the axial ligands for b_{566} heme (H78 and H173) and b_{560} heme (H92 and H187). Shown are the four mutations identified in the present study, Y268N, Y268C, L271V, and K272R, all in the quinone binding site II (Qo_2) of the protein. The three atovaquone resistance mutations we reported previously [4] are indicated, M133I and L144S in the quinone binding site I (Qo_1), and V284F in the sixth transmembrane domain. Shown in brackets are mutations reported in *P. falciparum*, i.e. M133I, Y268S, Y268N, Y268C, L271F, K272R, P275T, G280D, and V284F [6,11,12] Other *Plasmodium* atovaquone resistance mutations that had been reported [5,7,8] are indicated as grey shaded residues; in *P. yoelii* these mutations are I258M, F267I, Y268C, L271V and K272R.

mutations (M133I and K272R or P275T), or in transmembrane V284K [6]. The atovaquone resistance conferred by these mutations were between 10 and 100 times lower than that of the field isolates carrying the Y268S mutation. The degree of resistance correlated well with the concentration of atovaquone used in the isolation, and may explain the absence of mutations in codon 268 *in vitro*.

Amino acid residues Y268 and L271 are highly conserved, indicating the potential importance of these residues in maintaining the cytochrome *b* structure and function. Residue 272, on the other hand, is a lysine in *Plasmodium* spp., but is an arginine in vertebrate proteins. Both Y268 and L271 have been suggested to be involved in atovaquone binding in *P. falciparum* cytochrome *b* [6]. Furthermore, in the yeast model [13,14], residues 279 and 282, equivalent to *Plasmodium* residues 268 and 271, have been predicted to be involved in the binding of atovaquone. Site-directed mutagenesis resulting in Y279S and L282V in yeast (corresponding to Y268S and L271V in *Plasmodium*) indeed conferred atovaquone resistance [14].

The two codon 268 mutations found in the present study, Y268N and Y268C, lead to significantly different degrees of resistance (ED_{50} 80 and 5.2, respectively). The aromatic side-chain of the tyrosine at residue 268 is important for the interaction between atovaquone and its binding pocket in the cytochrome *b* [13,14]; site-directed mutations in yeast that remove the aromatic chain gave rise to atovaquone resistance. The substitution of this large hydrophobic residue with the smaller asparagine or cysteine would affect this interaction, and the difference in the polarity of the side chains of the two amino acids could explain the difference in degree of resistance conferred.

We found in the present study that the mutation at codon 271 was always associated with either K272R or M133I. The single mutation, L271V, may lead to a functionally defective structure that requires compensative mutations, either in the adjacent Qo_2 site, 272, or in Qo_1 site, 133, to restore stability. The significantly reduced growth rates of the various atovaquone resistant mutants indeed suggest that there is some disruption of the cytochrome *b* function. The mutations in the atovaquone binding domain could for example affect also the functional interaction between coenzyme Q and the cytochrome *b*. Further biochemical analyses of the *P. berghei* atovaquone resistant clones are in progress to elucidate the structure functional relationship underlying atovaquone resistance, and to examine the fitness of the mutant strains in genetic crosses.

Acknowledgments

The authors wish to thank Dr. Andy Waters, Leiden University Medical Center (LUMC), Netherland, and Dr. A. Kurniawan, Dept. of Parasitology, Faculty of Medicine, University of Indonesia for the gift of *P. berghei* ANKA strains.

This work was supported by a grant from the Indonesian government through the Ministry of Research and Technology and from the Japan Society for the Promotion of Sciences (JSPS) to JES, through a JSPS fellowship for PhD RONPAKU program. This study was also supported by a grant-in-aid for scientific research on Priority Areas, for the 21st Century COE Program (F-3) and for Creative Scientific Research from the Japanese Ministry of Education, Science, Culture, Sports and Technology (180 73004, 18GS0314).

References

[1] Fry M, Pudney M. Site of action of the antimalarial hydroxynaphthoquinone, 2-[trans-4-(4'-chlorophenyl)cyclohexyl]-3-hydroxy-1,4-naphthoquinone(566C80). Biochem Pharmacol 1992;43:1545–53.

[2] Vaidya AB, Lashgari MS, Pologe LG, Morrisey J. Structural features of *Plasmodium* cytochrome *b* that may underline susceptibility to 8-aminoquinolines and hydroxynaphthoquinones. Mol Biochem Parasitol 1993;58:33–42.

[3] Srivastava IK, Rottenberg H, Vaidya AB. Atovaquone, a broad spectrum antiparasitic drug, collapses mitochondrial membrane potential in a malarial parasite. J Biol Chem 1997;272:3961–6.

[4] Syafruddin D, Siregar JE, Marzuki S. Mutations in the cytochrome *b* gene of *Plasmodium berghei* conferring resistance to atovaquone. Mol Biochem Parasitol 1999;104:185–94.

[5] Srivastava IK, Morrisey JM, Darrouzet E, Daldal F, Vaidya AB. Resistance mutations reveal the atovaquone-binding domain of cytochrome *b* in malaria parasites. Mol Microbiol 1999;33:704–11.

[6] Korsinczky M, Chen N, Kotecka B, Saul A, Rieckmann K, Cheng Q. Mutations in *Plasmodium falciparum* cytochrome *b* that are associated with atovaquone resistance are located at a putative drug-binding site. Antimicrob Agents Chemother 2000;44:2100–8.

[7] Walker DJ, Wakefield AE, Dohn MN, Miller RF, Baughman RP, Hossler PA, et al. Sequence polymorphism in the *Pneumocystis carinii* cytochrome *b* gene and their association with atovaquone prophylaxis failure. J Infect Dis 1998;178:1767–75.

[8] McFadden DC, Tomavo S, Berry EA, Boothroyd JC. Characterization of cytochrome *b* from *Toxoplasma gondii* and Q_o domain mutations as a mechanism of atovaquone-resistance. Mol Biochem Parasitol 2000;108:1–12.

[9] Fivelman QL, Butcher GA, Adagu IS, Warhust DC, Pasvol G. Malarone treatment failure and *in vitro* confirmation of resistance of *Plasmodium falciparum* isolate from Lagos, Nigeria. Malaria J 2002;1:1–4.

[10] David KP, Alifrangis M, Salanti A, Vestergaard LS, Ronn A, Bygbjerg IB. Atovaquone/proguanil resistance in Africa: a case report. Scand J Infect Dis 2003;35:897–8.

[11] Musset L, Bouchaud O, Matheon S, Massias L, Le BJ. Clinical atovaquone–proguanil resistance of *Plasmodium falciparum* associated with cytochrome *b* codon 268 mutations. Microbes Infect 2006;11:2599–604.

[12] Schwöbel B, Alifrangis M, Salanti A, Jelinek T. Different mutation patterns of atovaquone resistance to *Plasmodium falciparum in vitro* and *in vivo*: rapid detection of codon 268 polymorphisms in the cytochrome *b* as potential *in vivo* resistance marker. Malaria J 2003;2:1–7.

[13] Kessl JJ, Lange BB, Merbitz-Zahradnik TM, Zwickers K, Hill P, Meunier B, et al. Molecular basis for atovaquone binding to the cytochrome bc_1 complex. J Biol Chem 2003;278:31312–8.

[14] Kessl JJ, Ha KH, Merritt AK, Lange BB, Hill P, Meunier B, et al. Cytochrome *b* mutations that modify the ubiquinol-binding pocket of the cytochrome bc_1 complex and confer anti-malarial drug resistance in *Saccharomyces cerevisiae*. J Biol Chem 2005;280:17142–8.

A Cryptic Algal Group Unveiled: A Plastid Biosynthesis Pathway in the Oyster Parasite *Perkinsus marinus*

Motomichi Matsuzaki,[*1] *Haruko Kuroiwa,*[†] *Tsuneyoshi Kuroiwa,*[†] *Kiyoshi Kita,*[‡] *and Hisayoshi Nozaki*[*]

*Department of Biological Sciences, Graduate School of Science, University of Tokyo, Tokyo, Japan; †Department of Life Science, College of Science, and Research Information Center for Extremophile, Rikkyo University, Tokyo, Japan; and ‡Department of Biomedical Chemistry, Graduate School of Medicine, University of Tokyo, Tokyo, Japan

Plastids are widespread in plant and algal lineages. They are also exploited by some nonphotosynthetic protists, including malarial parasites, to support their diverse modes of life. However, cryptic plastids may exist in other nonphotosynthetic protists, which could be important in studies on the diversity and evolution of plastids. The parasite *Perkinsus marinus*, which causes mass mortality in oyster farms, is a nonphotosynthetic protist that is phylogenetically related to plastid-bearing dinoflagellates and apicomplexans. In this study, we searched for *P. marinus* methylerythritol phosphate (MEP) pathway genes, responsible for de novo isoprenoid synthesis in plastids, and determined the full-length gene sequences for 6 of 7 of these genes. Phylogenetic analyses revealed that each *P. marinus* gene clusters with orthologs from plastid-bearing eukaryotes, which have MEP pathway genes with essentially the same mosaic pattern of evolutionary origin. A new analytical method called sliding-window iteration of TargetP was developed to examine the distribution of targeting preferences. This analysis revealed that the sequenced genes encode bipartite targeting peptides that are characteristic of proteins targeted to secondary plastids originating from endosymbiosis of eukaryotic algae. These results support our idea that *Perkinsus* is a cryptic algal group containing nonphotosynthetic secondary plastids. In fact, immunofluorescent microscopy indicated that 1 of the MEP pathway enzymes, 1-deoxy-D-xylulose 5-phosphate reductoisomerase, was localized to small compartments near mitochondrion, which are possibly plastids. This tiny organelle seems to contain very low quantities of DNA or may even lack DNA entirely. The MEP pathway genes are a useful tool for investigating plastid evolution in both of the photosynthetic and nonphotosynthetic eukaryotes and led us to propose the hypothesis that ancestral "chromalveolates" harbored plastids before a secondary endosymbiotic event.

Introduction

"Plastids" are intrinsic organelles in plants and algae, but gaps remain in our knowledge regarding their diversity and distribution. Plastids originally arose from endosymbiotic cyanobacteria and are now involved in processes including photosynthesis and other biochemical processes in plant cells. Among the protists, several lines of algae or plastid-bearing eukaryotes (PBEs), such as giant kelp and diverse bloom-forming algae are known. Furthermore, intracellular parasites of the phylum Apicomplexa, including the malarial parasite, have been recently shown to harbor nonphotosynthetic but essential plastids (Wilson 2005). In a very recent environmental sequencing study, a distinct group of PBEs, the picobiliphytes, were discovered (Not et al. 2007). Thus, it seems very likely that unknown PBEs still exist.

On the basis of their deduced evolutionary history, plastids can be divided into 2 classes: primary plastids with 2 bounding membranes, which are direct descendants of endosymbiotic cyanobacteria, and secondary plastids with more bounding membranes, which originate from past engulfed eukaryotic algae (Bhattacharya et al. 2004). Because secondary plastids remain "outside" with regard to membrane topology, proteins targeted to these compartments must be transported via a secretory pathway; they must contain an N-terminal bipartite targeting peptide, composed of a signal peptide (SP) to lead the polypeptide to the endoplasmic reticulum (ER), and a subsequent transit peptide (TP) to deliver the mature protein into the plastid lumen (van Dooren et al. 2001). Secondary PBEs are scattered over the protist phylogeny; however, it has been proposed that members of the so-called chromalveolate group, which consists of diatoms and other stramenopiles, haptophytes, cryptophytes, dinoflagellates, and apicomplexans, ancestrally contain secondary plastids of a single red algal origin (Cavalier-Smith 1999). Several lines of "evidence" support the "chromalveolate" hypothesis (Fast et al. 2001; Yoon et al. 2002), but critics note that the hypothesis assumes too many independent losses of plastids (Bodył 2005). Thus, a better understanding of plastid distribution in the basal chromalveolates is desirable to address these criticisms.

Perkinsus spp. are marine unicellular protists with a worldwide distribution that attack a wide range of mollusks, including clams and abalones, causing mass mortality (Villalba et al. 2004). *Perkinsus marinus* is the most notorious species of the genus because it parasitizes the eastern oyster *Crassostrea virginica* and has heavily impacted oyster fisheries and hence coastal water quality in the United States (Villalba et al. 2004). Molecular phylogenetic data have shown that this species is a basal chromalveolate derived from the ancestral dinoflagellates just after the split from apicomplexans (Cavalier-Smith and Chao 2004; Leander and Keeling 2004; Adl et al. 2005); thus, examining *P. marinus* for the existence of ancestral secondary plastids is of interest. Although electron microscopy (EM) observations have revealed no signs of plastids (Perkins and Menzel 1967; Perkins 1976, 1996; Sunila et al. 2001), 2 quite recent studies have suggested that *Perkinsus* spp. contain secondary plastids; *P. marinus* was shown to possess genes for a plant-type ferredoxin system that possibly encode plastid-targeting signals (Stelter et al. 2007) and an EM observation indicated a tiny organelle bounded by 4 membranes in *Perkinsus olseni* (=*Perkinsus*

[1] Present address: Department of Biomedical Chemistry, Graduate School of Medicine, University of Tokyo, Tokyo, Japan.

Key words: secondary endosymbiosis, protein sorting signal, chromalveolates, methylerythritol phosphate pathway, *Perkinsus marinus*.

E-mail: mzaki@m.u-tokyo.ac.jp

Mol. Biol. Evol. 25(6):1167–1179. 2008
doi:10.1093/molbev/msn064
Advance Access publication March 20, 2008

atlanticus) (Teles-Grilo et al. 2007). However, gene sequence or morphology in itself cannot prove the existence of vestigial plastids; at the least, localization data should be presented in order to confirm the presence of plastids.

Genome sequencing has revealed that biosynthesis of isoprenoid precursors is a key metabolic role of both photosynthetic (Matsuzaki et al. 2004; Derelle et al. 2006) and nonphotosynthetic (Gardner et al. 2002, 2005) plastids. Isoprenoids are a diverse and versatile group of compounds including sterols, carotenoids and other terpenes, and the side chains of quinones and chlorophylls. Isoprenoids are all derived from isopentenyl diphosphate and its isomer, both of which are synthesized by the methylerythritol phosphate (MEP) pathway in plastids but the mevalonate (MVA) pathway in the cytosol of many eukaryotes, including higher plants and animals (Rodríguez-Concepción 2004). It has been suggested that in eukaryotes the MEP pathway only exists in PBEs, with a discussion of the evolutionary origins of the genes based on the orthologs of higher plants and several bacteria, although only 5 out of 7 MEP genes were known at the time (Lange et al. 2000). Many eukaryotic genomes have been sequenced since then, and to date the MEP pathway genes have been found to be specific to PBEs and would seem to be necessary for most given that they lack the MVA pathway genes; thus, it seems that the MEP pathway is a specific feature of plastids, photosynthetic, or otherwise. Therefore, the 7 MEP pathway genes (shown in fig. 1) would be good molecular markers for the study of plastid distribution and evolutionary history; however, to the best of our knowledge, no prior studies have involved the widespread sampling of PBEs.

A preliminary database of the *P. marinus* genome at The Institute for Genomic Research (TIGR) contains partial sequences of the MEP pathway genes (the existence of ispC, ispG, and ispH has already been discussed by Stelter et al. [2007]). In this study, we attempted to clone full-length MEP pathway genes of *P. marinus* to elucidate the evolution of secondary plastids by phylogenetic analyses. A new analytical method for investigating protein sorting signals was also developed to compare signals between genes. Finally, immunofluorescent microscopy was performed to demonstrate the existence of plastids in *P. marinus*.

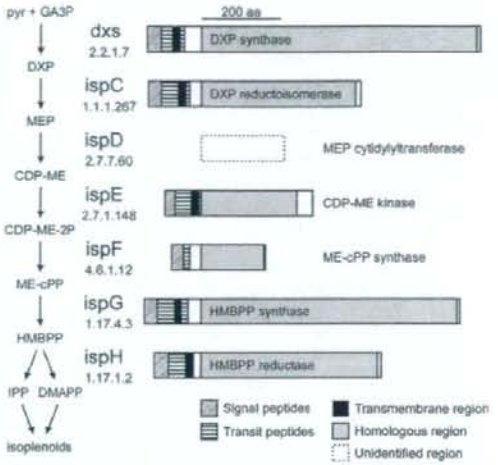

FIG. 1.—The MEP pathway and responsible genes in *Perkinsus marinus*. The flowchart on the left shows the compounds and reactions involved in the MEP pathway, with the name of the gene responsible and an Enzyme Committee number listed for each reaction. Compounds are abbreviated as follows: pyr, pyruvate; GA3P, glyceraldehyde 3-phosphate; DXP, 1-deoxy-D-xylulose 5-phosphate; MEP, 2-*C*-methyl-D-erythritol 4-phosphate; CDP-ME, 4-diphosphocytidyl methylerythritol; CDP-ME-2P, CDP-ME 2-phosphate; ME-cPP, methylerythritol 2,4-cyclodiphosphate; HMBPP, 1-hydroxy-2-methyl-2-butenyl 4-diphosphate; IPP, isopentenyl diphosphate; and DMAPP, dimethylallyl diphosphate. On the right are schematic representations of the inferred structures of MEP pathway enzymes in *P. marinus*. N-terminal extensions that were putatively composed of SP (diagonal hatch) and TP (horizontal stripe) with a transmembrane region (filled) were located next to the regions that were homologous to each enzyme's bacterial counterpart (shaded). The gene for the third step, an *ispD* ortholog, is unidentified and indicated by a box with dotted edges. The scale is indicated at the top of the figure.

Materials and Methods

Culture Conditions

Perkinsus marinus strain CRTW-3HE was obtained from the American Type Culture Collection (number 50439; ATCC, Manassas, VA) and maintained at 26 °C in ATCC Medium 1886. Discontinued products for the medium components were substituted as follows during the course of the study: Instant Ocean Sea Salt (Aquarium Systems, Mentor, OH) for artificial seawater (S1649; Sigma, St Louis, MO) and Lipid Mixture (1000×; L5146; Sigma) for Lipid Concentrate (100×; 21900-014; Gibco, Grand Island, NY).

Sequencing MEP Pathway Genes

Total RNA was extracted from cell pellets using TRIzol Reagent (Invitrogen, Carlsbad, CA), and the mRNA was enriched using the PolyATtract mRNA Isolation System III (Promega, Madison, WI). Complementary DNA was synthesized using the CapFishing Full-length cDNA Premix Kit (Seegene, Seoul, Korea) with random hexamers or the oligo dT adapter as a primer. Reverse transcriptase–polymerase chain reaction and rapid amplification of cDNA ends were performed using PrimeSTAR HS DNA polymerase (Takara Bio, Tokyo, Japan) and the primers listed in supplementary table S1 (Supplementary Material online). Polymerase chain reaction products were purified using Wizard SV Gel and PCR Clean-Up System (Promega) and then cloned with the ZeroBlunt TOPO PCR Cloning Kit for Sequencing (Invitrogen). Inserts were sequenced using vector-specific or gene-specific (shown in supplementary table S1, Supplementary Material online) primers. Full-length sequences have been deposited in DDBJ/EMBL/GenBank under the accession numbers AB284361–AB284366 (shown in supplementary table S3, Supplementary Material online). All experiments described here were performed according to the manufacturers' instructions. The amino acid sequences were inferred from the most upstream ATG with the universal codon table.

Phylogenetic Analysis

All possible MEP pathway orthologs for bacteria for which complete genome sequences were available as of 1